Int. J. Mol. Sci. **2002**, *3*, 276-309

International Journal of
Molecular Sciences
ISSN 1422-0067

www.mdpi.org/ijms/

Chemical Reactivity as Described by Quantum Chemical Methods

P. Geerlings[*] and F. De Proft

Eenheid Algemene Chemie, Free University of Brussels (VUB), Pleinlaan 2,1050 Brussels,Belgium
Tel: +32. 2.629 33 14, Fax: +32.2. 629 33 17, e-mail: pgeerlin@vub.ac.be
[*] Author to whom correspondence should be sent

Received: 28 September 2001 / Accepted: 7 January 2002 / Published: 25 April 2002

Abstract: Density Functional Theory is situated within the evolution of Quantum Chemistry as a facilitator of computations and a provider of new, chemical insights. The importance of the latter branch of DFT, conceptual DFT is highlighted following Parr's dictum "to calculate a molecule is not to understand it". An overview is given of the most important reactivity descriptors and the principles they are couched in.

Examples are given on the evolution of the structure-property-wave function triangle which can be considered as the central paradigm of molecular quantum chemistry to (for many purposes) a structure-property-density triangle. Both kinetic as well as thermodynamic aspects can be included when further linking reactivity to the property vertex. In the field of organic chemistry, the ab initio calculation of functional group properties and their use in studies on acidity and basicity is discussed together with the use of DFT descriptors to study the kinetics of S_N2 reactions and the regioselectivity in Diels Alder reactions. Similarity in reactivity is illustrated via a study on peptide isosteres. In the field of inorganic chemistry non empirical studies of adsorption of small molecules in zeolite cages are discussed providing Henry constants and separation constants, the latter in remarkable good agreement with experiments. Possible refinements in a conceptual DFT context are presented. Finally an example from biochemistry is discussed : the influence of point mutations on the catalytic activity of subtilisin.

Keywords: Conceptual DFT, Quantum Biochemistry, Zeolites, Organic Reactivity, Quantum Similarity.

---

1. Quantum Mechanics, Quantum Chemistry, Computational Chemistry, Density Functional Theory: who is who

1.1. From Quantum Mechanics to Quantum Chemistry and Computational Chemistry

The failure of classical physics (mechanics and electromagnetism) at the end of the 19th century led to the introduction of the Quantum Concept by Planck, Einstein, Bohr,... culminating in the birth of "modern" quantum mechanics around 1925 due to the work of Schrödinger, Heisenberg, Born, … Schrödinger's equation occupied a central position in this new theory and, although later on complemented by its relativistic analogue by Dirac, stood the test of time and has been for now 75 years the central equation for the description both of the internal structure of atoms and molecules and their interactions. In his famous quote Dirac already in 1929 went so far to state [1] "The underlying physical laws necessary for the mathematical theory of a large part of physics and the whole of chemistry are thus completely known, and the difficulty is only that the exact application of these laws leads to equations too complicate to be soluble."

The step from Quantum Mechanics to Quantum chemistry can in principle be situated in the pioneering work by Heitler and London [2] on the hydrogen molecule in 1928 providing insight into, to quote Pauling, the Nature of the Chemical Bond [3]. However Quantum Chemistry is, at least in our opinion, more than the mere application of quantum mechanical principles to molecules and their interaction. In the years between 1930 and 1950 Pauling [3], Huckel [4], Coulson [5] indeed used quantum mechanical principles but combined them with their chemical intuition thereby gradually creating a new discipline, nowadays called Quantum Chemistry. The Valence Bond approach (after Heitler and London) was prominent in those days, to the detriment of Hund's and Mulliken's MO method [6]. A revolution was provoked by Roothaan's matrix formulation of the MO method in 1951 [7]. Its elegance together with the increasing computer power paved the way for the large scale introduction of the MO-LCAO method within the framework of the Hartree Fock Self Consistent Field (SCF) approach [8a] as excellently summarized in Pople's comprehensive treatise [8b].

The late seventies, eighties and nineties saw the development and/or the adaptation for systematic use of beyond SCF methods including (part of) electron correlation: Møller Plesset Perturbation Theory [9], the method of Configuration Interaction [10] and various types of Coupled Cluster Theory [11]. The introduction of initially freely distributed, later on commercially available, computer programs which became more and more user friendly (cf Pople's GAUSSIAN series) [12] definitely promoted Quantum Chemistry, from a branch of Theoretical Chemistry almost exclusively reserved for "pure-sang" theoreticians and concentrating on diatomic and small polyatomic molecules, to a field also creating tools for non-specialists, in many other subfields of Chemistry (Inorganic, Organic, Biochemistry). The new subfield "Computational Chemistry" with P. Schleyer as a prominent figure [13] particularly stresses the "applied" aspects of Quantum Chemistry.

The combination of conceptual and methodological improvements, and the growing performance of soft- and hardware led to an ever increasing accuracy in the treatment of problems of a given complexity. Orders of magnitude in the complexity.of problems that could be treated at a given level were gained. These evolutions are beautifully illustrated in Pople's two dimensional chart of Quantum Chemistry, given below in Figure 1 in a slightly adapted version [14].

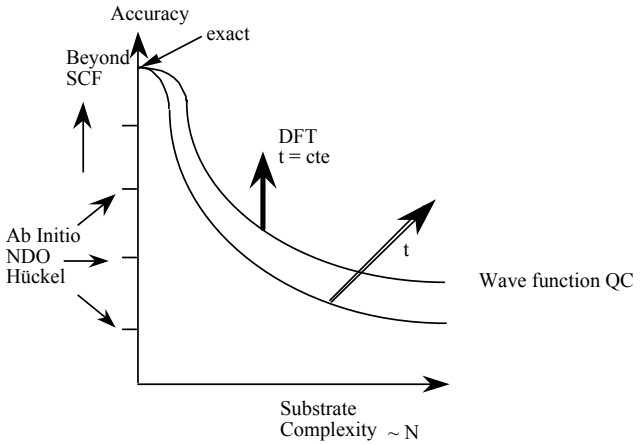

Figure 1: Accuracy versus complexity chart of Quantum Chemistry (After J.A.Pople)

A central paradigm in Quantum Chemistry is the Structure-Properties-Wave function triangle(Fig.2), Structure and Properties further determining reactivity. The third corner of the triangle is the ground state wave-function Ψ_o,or more generally also all excited state wavefunctions determining all properties of the system.

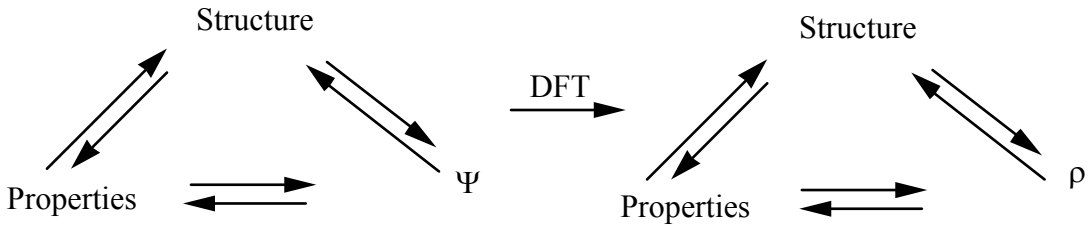

Figure 2 : The central paradigm in Quantum Chemistry and its evolution upon the introduction of DFT

1.2. Density Functional Theory revolutionarized Quantum Chemistry from a computational point of view

A step of immense importance has been taken by Kohn and Hohenberg [15] in 1964. They proved that the information content in the electron density function $\rho(r)$, depending on only 3 variables, determines all ground state properties, thus replacing the crucial position of the complex wavefunction, Ψ ,function of 4N variables (where N is the number of electrons).

Equation (1) clearly shows how much information in the wave function of a N-electron system is integrated out when passing to the electron density (x stands for a four vector containing three spatial coordinates r and one spin coordinates of an electron) [16]

$$\rho(\underline{r}) = N\int \Psi^{*}(\underline{x}, \underline{x}_2, \underline{x}_3 \ldots, \underline{x}_N)\,\Psi(\underline{x}, \underline{x}_2, \underline{x}_3, \ldots, \underline{x}_N)\,d\underline{s}\,d\underline{x}_2\,d\underline{x}_3 \ldots d\underline{x}_N \qquad (1)$$

The problem of searching an optimal ρ instead of the much more complex optimal Ψ is most conveniently done within the Kohn-Sham formalism [17]) introducing orbitals φ_i, whose squares sum up to the electron density.

$$\rho = \sum_i |\varphi_i|^2 \qquad (2)$$

A variational procedure yields a pseudo-one electron equation, the analogue of the Hartree-Fock equations, which is written as

$$\left(-\frac{1}{2}\nabla_i^2 + v(\underline{r}) + \int \frac{\rho(\underline{r})}{|\underline{r} - \underline{r}'|}\,d\underline{r} + v_{xc}(\underline{r})\right)\varphi_i = \varepsilon_i \varphi_i \qquad (3)$$

Here, besides the electronic kinetic energy term ($-\frac{1}{2}\nabla_i^2$), the nuclear attraction term $v(\underline{r})$ and the classical electronic repulsion term, the exchange correlation term $\upsilon_{xc}(\underline{r})$ appears whose form is actually unknown. One of the key features of present day DFT is the search for the best performing exchange correlation functionals [18]. Although this task is hampered by the lack of a unifying principle as present in wave-function theory (see e.g. Pople's Model Chemistry chart) [8b] impressive progress has been made in recent years among others via the so called hybrid functionals [19] which gained widespread use. Extensive testing of their capability in reproducing molecular properties has been performed [20, 21]. The whole of these efforts led to a methodology which affords the calculation of molecular ground state properties of high quality (in fact often way beyond SCF) at a much lower computational cost. Parr and Yang termed this branch of DFT "Computational DFT" [18]. A "témoignage par excellence" of the ever increasing importance of DFT is (the title of) Koch's book "A Chemist's Guide to DFT" [22] published in 2000 offering an overview of the performance of DFT for various properties to the practicing organic or inorganic chemist. As a result of this evolution the triangle is Fig. 2 can be adapted at one of its vertices, putting ρ (and its obtention via computational DFT) at equal footing with the wave-function Ψ.

1.3. DFT as a provider of new insights : conceptual DFT

1.3.1. From computational chemistry to chemical insight

Both wave function Quantum Chemistry and Density Functional Theory, when being used to compute atomic and molecular properties, yield results which often and for most chemists are not always directly exploitable. The numbers they produce should in many cases be translated, or casted

into a language or formalism pointing out their chemical relevance. As simply stated by Parr [23] "Accurate calculation is not synonymous with useful interpretation. To calculate a molecule is not to understand it". Quite often this translation involves terms going back to the early days of theoretical chemistry but still in use as a guideline for chemists in the interpretation of experimental data: hybridization, electronegativity, aromaticity, …

A beautiful example in wave function quantum chemistry, dating from the sixties and seventies is the transformation of the Molecular Orbitals resulting from the Hartree-Fock equations, which are, usually delocalized over the entire molecule, to a set of localized Molecular Orbitals using a localization criterion [24]. The resulting MO picture is much closer to the Lewis picture of great use in organic chemistry (Figure 3), e.g. in the study of the electronic structure of bonds and its relation to spectroscopic properties. The relation between NMR coupling constants and the percentage of s character of the carbon atom hybrid involved in a CH bond [27], is a classical example, partly addressed in our own work [28]. Of importance in both branches (wave function and Density Functional Theory) is the visualization of the results (e.g. electron density or density difference plots (as in Figure 3), its extensive use also going hand in hand with hard- and software developments.
Also in this area of obtaining a better chemical insight via Quantum Chemical calculations, a prominent role was played in recent years by DFT.

1.3.2. DFT as a source of Chemical Concepts

As already mentioned before, computational DFT is founded on a variational principle, more precisely for the energy functional

$$E = E[\rho] \tag{4}$$

Looking for an optimal ρ, i.e. the one which minimizes E, is thereby subjected to the constraint that ρ should at all times integrate to N, the number of electrons.

$$\int \rho(\underline{r}) d\underline{r} = N \tag{5}$$

Within a variational calculation this constraint is introduced via the method of Lagrangian multipliers, yielding the variational condition

$$\delta[E - \mu\rho] = 0 \tag{6}$$

where μ is the Lagrangian multiplier, a constant gaining its physical significance in the differential equation (the Euler equation) resulting from (6)

$$v(\underline{r}) + \frac{\delta F_{HK}}{\delta \rho} = \mu \tag{7}$$

Here $v(\underline{r})$ is the external potential (i.e. due to the nuclei) and F_{HK} is the Hohenberg Kohn functional containing the electronic kinetic energy and the electron-electron interaction operators [29]. It has been Parr's impressive contribution to identify this abstract Lagrange multiplier as [30]

$$\mu = \left(\frac{\partial E}{\partial N}\right)_v = -\chi \tag{8}$$

i.e. the derivative of the energy of the atom or molecule with respect to its number of electrons at constant external potential (i.e. identical nuclear charges and positions) (Figure 4). In this seminal

paper, cited already more than 500 times, Parr thereby regained Iczkowski and Margrave's definition of electronegativity $(\chi = -\partial E/\partial N)$ [31], Mulliken's 1934 definition

$$\chi = \frac{1}{2}(IE + EA) \tag{9}$$

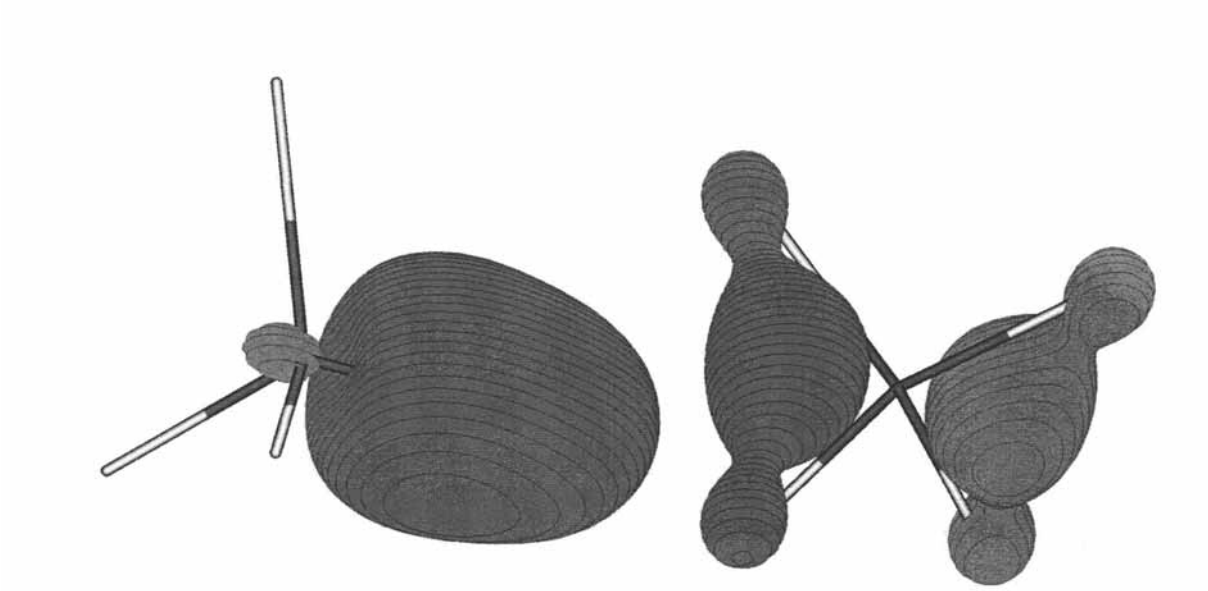

Figure 3 : Delocalized Hartree Fock versus Localized Orbitals : one of the triply degenerate HOMO orbitals of methane versus a CH bond orbital. Electron density plot (Hartree Fock STO-3G/Boys localization procedure [25]) obtained with the software package [26]

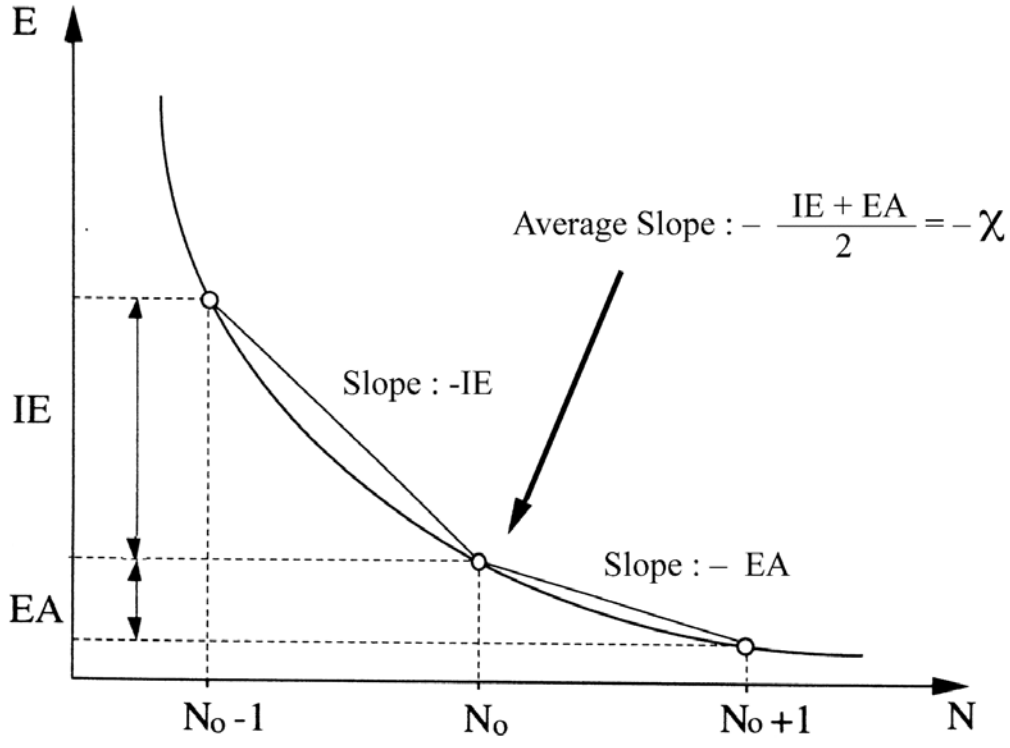

Figure 4 : Atomic or molecular energy (E) versus number of electrons (N) at constant external potential : the modern definition of electronegativity

can be considered as an approximation to it [32]. The Mulliken values, the arithmetic average of ionization energy (IE) and electron affinity (EA), were already shown before to correlate with the Pauling values [33] and received more and more importance in recent years on the basis of its simpler foundation. It can easily be seen that they correspond to the average slope of the E=E(N) curve at the N value considered.

In analogy with the thermodynamic potential

$$\mu_{\text{Therm}} = \left(\partial G \big/ \partial n\right)_{P,T} \tag{10}$$

where G represents the Gibbs Free Energy function and n the number of moles, μ was termed electronic chemical potential which turns out to be the negative of the electronegativity.

Within a few years after Parr's contribution various other quantities representing the response of a system's energy to perturbation in its number of electrons and/or its external potential (cf the index v in 8), which both lie at the heart of chemistry, were published. They can nicely be ordered according to Nalewajski's charge sensitivity analysis [34] (Figure 5).

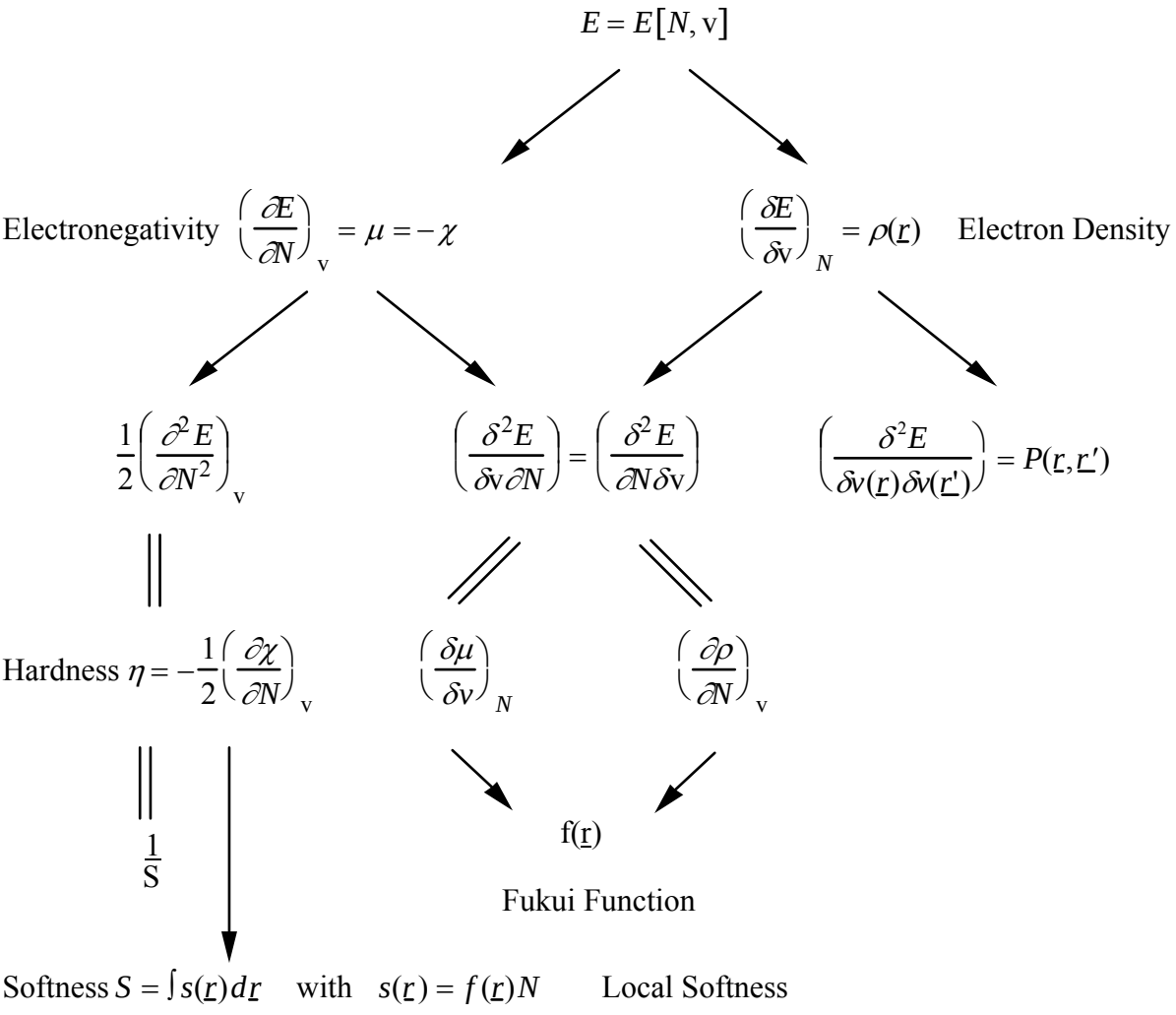

Figure 5 : Nalewajski's Sensitivity Analysis : atomic and molecular properties as energy derivatives with respect to N and v.

Appearing in a natural way are

-the chemical hardness η, an identification proposed by Parr and Pearson [35] for the second derivative which respect to N, $\left(\frac{\partial^2 E}{\partial N^2}\right)_v$, and representing the resistance of a system to changes in its number of electrons. The chemical softness S is naturally defined as the inverse of η

$$S=1/2\,\eta \qquad (11)$$

The analogue of equation (9) turned out to be

$$\eta=\frac{1}{2}(IE-EA) \qquad (9')$$

-the Fukui function f(r) [36], representing the change in electron density ρ at a given point r when the total number of electrons is changed, a generalization of Fukui's frontier orbital concept [37]

-a local version of S, s(r), obtained by multiplying S and f(r), the latter function distributing the local softness over various domains in space [38]

(Other concepts introduced in this framework are reviewed in [39, 40])

In this way it is shown that DFT gave the possibility to sharply define concepts known for a long time in chemistry, but to which inadequate precision could be given to use them with confidence in quantitative studies.

The last 15 years showed growing importance of this branch of DFT, conceptual DFT, where these concepts were used as such or within the context of three important principles,

-Sanderson's electronegativity equalization principle [41, 42] stating that upon molecule formation, atoms (or more general arbitrary portions of space of the reactants) with initially different electronegativities $\chi_i^o (i=1,....,M)$ combine in such a way that their "atoms-in-molecule" electronegativities are equal. The corresponding value is termed the molecular electronegativity χ_M. Symbolically :

$$\chi_1^o,\ \chi_2^o,\ ....,\ \chi_M^o \longrightarrow \chi_1 = \chi_2 = ... = \chi_M$$

isolated atoms molecule formation

Electron transfer thereby takes place from atoms with lower electronegativity to those with higher electronegativity, the latter reducing their χ value, the former increasing it (Fig.6)

-Pearson's Hard and Soft Acids and Bases Principle (HSAB) [43, 44] stating that Hard (Soft) Acids (electron pair acceptors), preferentially interact with hard (soft) Bases (electron pair donors).

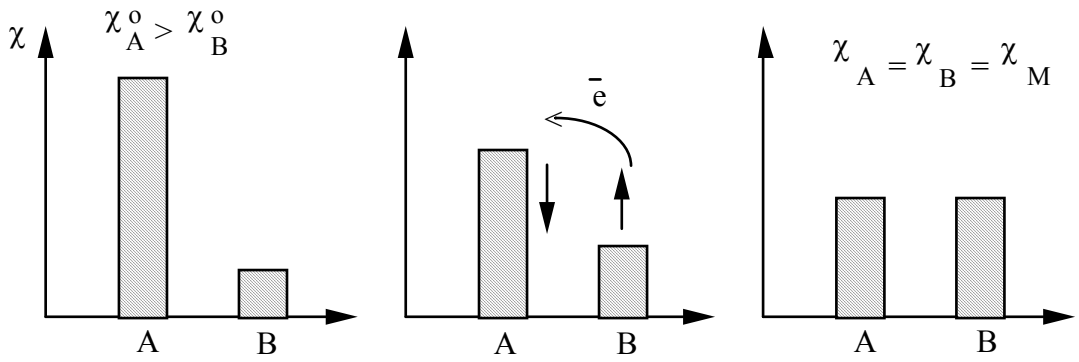

Figure 6 : Sanderson's Electronegativity Equalization Principle

Both principles were proven [30, 45] as was also the third one, the Maximum Hardness Principle, stating "that molecules try to arrange themselves to be as hard as possible" [44, 46].
In recent years our group was active in the development and/or use of DFT based concepts as such or within the context of the afore mentioned and other principles. Also performance testing was one of our objectives : setting standards for computational DFT in order that it can be used for a given type of problem with the same level of confidence as the combination of level and basis set in the case of Pople's model Chemistry for wave function theories. Studies were undertaken on IR frequencies and intensities, dipole and quadrupole moments, ionization energies and electron affinities and Molecular Electrostatic Potentials [20, 47,48,49].

2. The structure -property (reactivity)- electron density triangle: some examples

2.1. Introduction

In this second part of the contribution examples are given on the role DFT studies, both conceptual and computational, can play in exploiting the structure, property -density triangle in Fig. 2 where we concentrate on properties directly related to reactivity (both seen from a thermodynamic and kinetic point of view). Examples will be taken essentially from our own work with reference to work of other groups if relevant to the discussion. As such this part is not aiming at completeness at all. The reader should consult other sources to have a complete overview of applications of conceptual DFT [39, 40a, 40b]. Illustrations will be taken from organic, inorganic and biochemistry.

2.2. Organic Chemistry

2.2.1. Group properties and their use in acidity and basicity studies

Functional groups are playing a fundamental role in rationalizing structure and reactivity, thus dictating transformations in synthetic chemistry [50], both in organic and inorganic chemistry. An

insight in the properties of these molecular building blocks is of utmost importance in the design of a rational chemistry.

Whereas group electronegativity has already a longstanding history [33], the field of group softness and/or hardness is much less developed. Moreover a non-empirical uniform computational scheme obeying the working equations (9) and (9') was lacking in the period we started this work.

We therefore presented a non-empirical computational scheme for group electronegativity, hardness and softness [51] for more than 30 functional groups

CH_3 ; CH_2CH_3; $CH{=}CH_2$; $C{\equiv}CH$; CHO ; $COCH_3$; COOH ; COCl ; $COOCH_3$; $CONH_2$; $C{\equiv}N$; NH_2 ; CH_2-NH_2 ; NO_2 ; OH ; CH_2OH ; OCH_3 ; F ; CH_2F ; CHF_2 ; CF_3 ; SiH_3 ; PH_2 ; SH ; CH_2SH ; SCH_3 ; Cl ; CH_2Cl ; $CHCl_2$; CCl_3.

Starting from the geometry the group usually adopts when being embedded in the molecule we calculated its η,S and χ values via (9) and (9'), considered as a radical, both at the Hartree Fock and CISD level using Pople's 6-31++G** basis [8b]. Figure 7 shows the correlation of the CISD calculated group electronegativities (showing a correlation coefficient r of 0.943 with the HF values for the same basis) with what is recently [52] considered as the most appropriate "experimental scale", the ^{13}C $^{1}J_{CC}$ (ipso ortho) coupling constants in monosubstituted benzenes [53]. As can be seen the correlation fails for OCH_3 and SiH_3 for reasons that could not be detected. It is less convincing for groups containing triple bonds clearly to the higher demands for correctly describing electron correlation effects. Dropping these values a correlation coefficient r of 0.941 is obtained for the remaining groups.

Typical trends to be observed are

- the central atom effect

  $\chi_{CH_3} < \chi_{NH} < \chi_{OH}$ cf. $\chi_C < \chi_N < \chi_O$

  indicating that upon saturation of two different atoms with hydrogens the electronegativity of the resulting groups parallels that of the naked atoms.

- the second row effect

  $\chi_{CH_3} > \chi_{SiH_3}$

  $\chi_{NH_2} > \chi_{PH_2}$

  $\chi_{OH} > \chi_{SH}$

showing increasing electronegativity of a group the higher the central atom is positioned in a given column of the periodic table.

- the hybridisation effect

  $\chi_{CH_2CH_3} < \chi_{CH=CH_2} < \chi_{C+CH}$

  $\chi_{CH_2NH_2} < \chi_{CH=NH_2} < \chi_{C+N}$

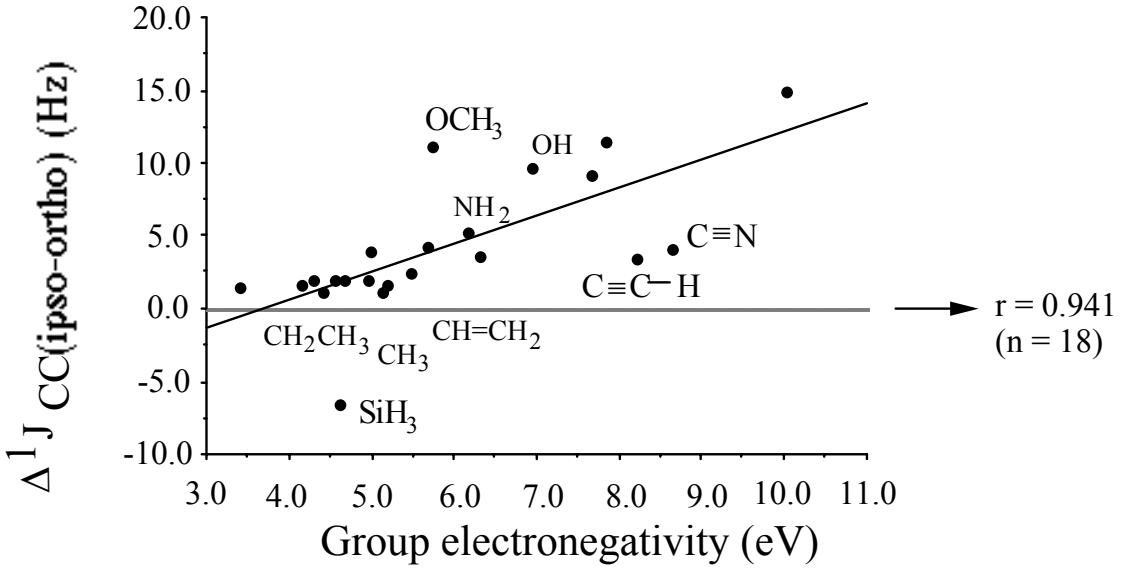

Figure 7 : Calculated vs. Experimental Group Electronegativity values.

indicating increasing electronegativity upon increasing s-character of the central atom of the group.

For alkylgroups the intuitively expected decrease of χ upon increasing chain length or branching is found : Me : 5.12 ; Et : 4.42 ; n-Pr : 4.39 ; i-Pr : 3.86 (CISD values).

Turning now to the hardness values, experimental scales are scarce, the best candidate being the corresponding radical hardness [54], although possible differences in geometry (e.g. for the CH_3 radical) indicate that this correlation should be looked upon with much reserve. Figure 8 shows a correlation, upon withdrawing the extremely hard CF_3 group as an outlier, of 0.926 for the 14 remaining cases for which experimental values are available. Typical trends which can be discussed are again (vide supra)

- the central atom effect

  $\chi_{CH_3} < \chi_{NH_2} > \eta_{OH} < \eta_F$ cf. $\eta_C < \eta_N > \eta_O < \eta_F$

- the second row effect (extremely important in forthcoming discussions but here already illustrating the opposite behaviour of χ and S)

  $\eta_{OH} > \eta_{SH}$

  $\eta_{CCl_3} < \eta_{CH_3} < \eta_{CF_3}$

  $\eta_{CH_3} > \eta_{SiH_3}$

- the "volume" effect in alkyl groups, showing decreasing hardness (increasing softness) upon increasing chain length or branching. CISD η values illustrating this trend are

  6.60 (H) ; 5.34 (Me) ; 4.96 (Et) ; 4.70 (n-Pr) ; 4.62 (i-Pr)

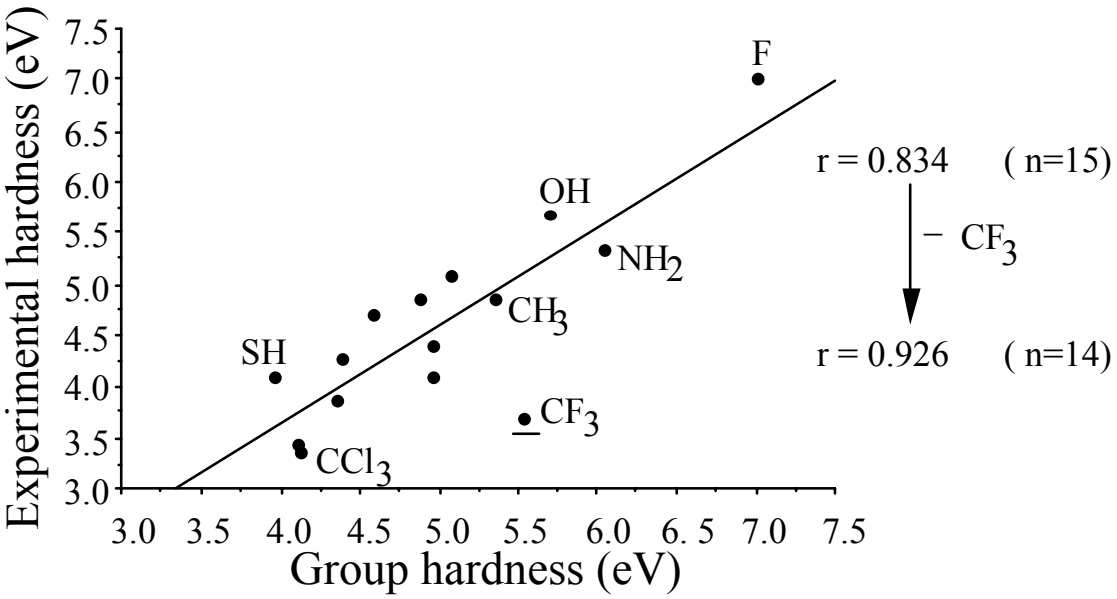

Figure 8 : Calculated vs. Experimental Group Hardness values (see text).

As an example of the use of group properties we consider [55] the experimental acidity sequence of alkylalcohols showing an opposite behaviour in aqueous solution and gas phase [56] [57]. Whereas in aqueous solution the acidity decreases upon increasing carbon chain length and branching, the opposite behaviour is encountered in the gas phase. The former trend is usually traced back to the electron donating character of alkylgroups (the +I effect as well known in electrophilic aromatic substitutions on benzene [58]), whereas the latter tendency should imply an at first sight unexpected electron withdrawing character of alkyl groups.

We correlated the (gas phase) acidity quantified by the $\Delta G°_{acid}$ value with the calculated alkylgroup properties χ and η (all calculations were done at a uniform 6-31G* MP4 level). The sequences parallel those of the 6-31++G** CISD values in [51].

The values shown in Table 1 indicate the expected tendencies of increasing softness upon increasing chain length and branching accompanied by decreasing electronegativity, reflecting the traditional idea of an alkylgroup as electron donor (+I effect). It was tempting to have a more detailed look at the correlation between charge distribution, both in the acidic form ROH and the alkoxide anion RO^-, and the acidity variation upon varying R. We therefore made use of χ and η values given in Table 1 with an electronegativity equalization scheme.

Working at functional group resolution and neglecting external perturbation higher order terms one obtains that upon embedding a functional group A with intrinsic χ_A^0 and η_A^0 into a molecule its electronegativity changes to χ_A with

$$\chi_A = \chi_A^0 - 2\eta_A^0 \Delta N_A \qquad (11)$$

Table 1. 6-31G* MP4 alkylgroup properties : electronegativity χ (eV) and hardness η (eV)

	χ	η
Me	4.35	5.98
Et	3.76	5.45
n-Pr	3.68	5.17
i-Pr	3.44	5.04
n-Bu	3.57	5.05
t-Bu	3.30	4.19

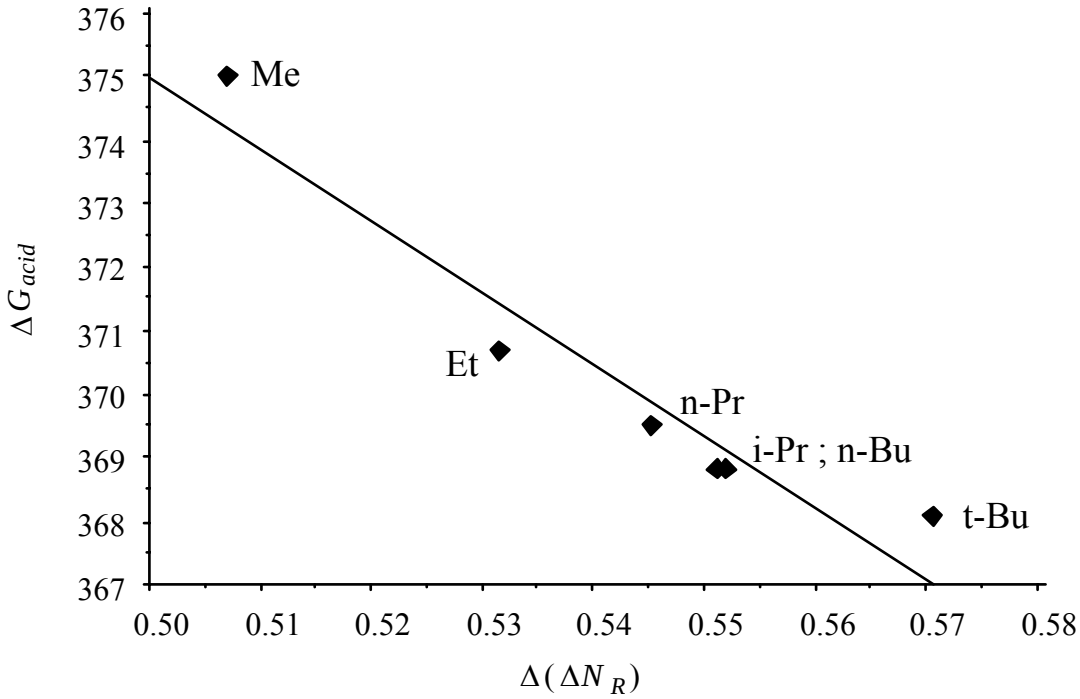

Figure 9 : Experimental gas phase acidity of alkylalcohols (in kcal mol^{-1}) vs. $\Delta(\Delta N_R)$ (see text) (reprinted with permission by Pergamon/Elsevier-Reference [55]).

This equation is easily derived using a Taylor series expansion of the E = E[N,v] functional (cf. Fig.5) around a reference number of electrons and at constant external potential. Applying this relationship to both the acidic form of an alcohol ROH both for the R and OH groups and equalizing the electronegativities of both molecular building blocks, one gets for ΔN_{R_I} (the number of electrons transferred to the alkylgroup in the acidic form)

$$R{:}OH \qquad \Delta N_{R_I} = \frac{\chi_R^0 - \chi_{OH}^0}{2\left(\eta_R^0 + \eta_{OH}^0\right)} < 0 \qquad (12)$$

In the case of the conjugate base RO^- one obtains in a completely analogous way (taking into account again charge conservation, but now not at charge 0 but -1)

$$R{:}O^{-} \qquad \Delta N_{R_{II}} = \frac{\chi_R^0 - \chi_O^0}{2\left(\eta_R^0 + \eta_O^0\right)} + \frac{\eta_O^0}{\eta_R^0 + \eta_O^0} \qquad (13)$$

(a) (b)

In (12) ΔN_{R_I} is negative as χ_{OH} is higher than χ_R^0 in the case of an alkylgroup. The intramolecular charge transfer is electronegativity dominated, as far as its direction is concerned, hardness playing a role in the amount of charge transferred. In the conjugate base form eqn.(13) indicates that a second, completely hardness-determined term, shows up which turns out to be larger in absolute value than the first term in all cases considered. This hardness dominated term consequently accounts for an electron transfer towards the alkyl group, the value being more important when the softness of the alkylgroup increases. Equating η^0 and χ^0 both for OH and O, the difference between $\Delta N_{R_{II}}$ and ΔN_{R_I} , $\Delta(\Delta N_R)$, can be approximately written as

$$\Delta\left(\Delta N_R\right) = \Delta N_{R_{II}} - \Delta N_{R_I} \approx \frac{\eta_O^0}{\eta_R^0 + \eta_O^0} \qquad (14)$$

indicating that the difference in electron transfer from R to the oxygen part of the alcohol upon deprotonation becomes more important when the alkylgroup is softer. Otherwise stated : $\Delta(\Delta N_R)$ is R-softness dominated. It may be therefore concluded that in order to correctly describe acid-base properties of molecules, the electronic properties of the charged form of the acid base equilibrium are of utmost importance. Figure 9 shows the excellent correlation between the experimental gas phase acidity and $\Delta(\Delta N_R)$ for the simplest alkylalcohols. In the present case alkylgroups act as electron acceptors; these electron withdrawing properties of alkylgroups were previously encountered in the literature in cases where alkylgroups are placed on negatively charged carbon atoms or reaction centers such as in α-alkylbenzyl carbanions [59].

We finally turned to the effect of solvent. We therefore recalculated group electronegativity and softness values, using a Self Consistent Reaction Field Model [60], introducing the solvent dielectric constant ε [61]. In Figure 10 we plot the $\Delta(\Delta N)$ quantity as a function of the Kirkwood function $\frac{\varepsilon - 1}{2\varepsilon + 1}$ related to the free energy of solvatation.

It is seen that an approximate linear relationship between $\Delta(\Delta N)$ and the Kirkwood function is found for the simplest alkylalcohols, with a crossing of the curves near the H_2O case. The gas phase acidity sequence is thereby inverted when passing to aqueous solution as found experimentally [62].

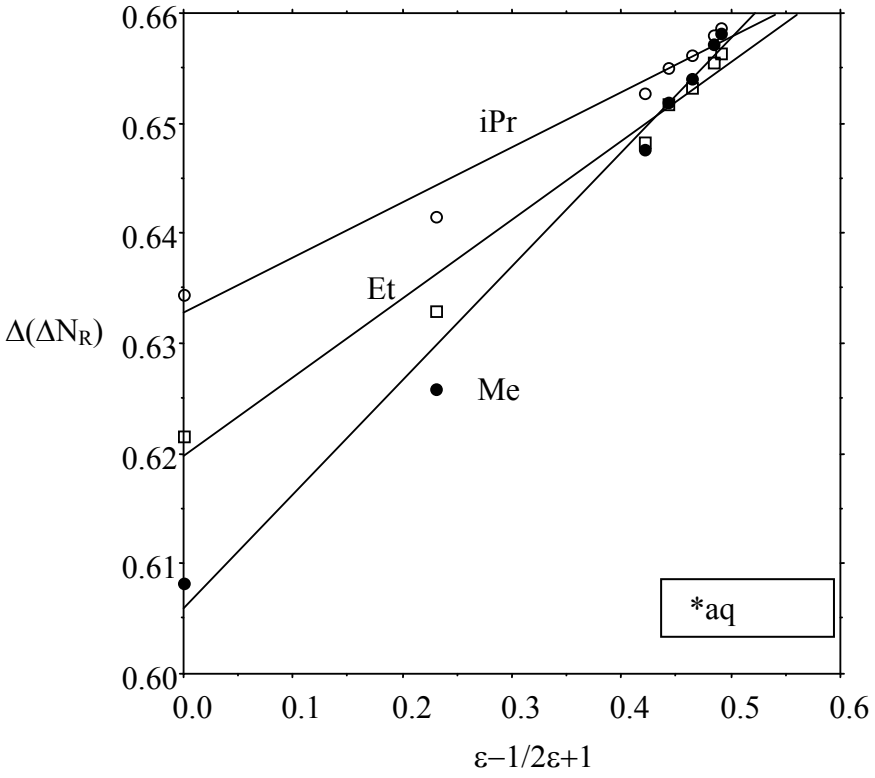

	ε
Gas phase	0
Benzene	2.28
CH_2Cl_2	8.93
Pyridine	12.4
Acetone	20.70
DMSO	46.68
H_2O	78.39*

Figure 10. Plot of $\Delta(\Delta N_R)$ versus the Kirkwood function $\frac{\varepsilon - 1}{2\varepsilon + 1}$ (Reprinted with permission by the American Chemical Society - Reference [61]).

2.2.2. Kinetics of S_N2 reactions

The nucleophilic substitution reaction is one of the basic transformations in organic chemistry. It has been extensively studied both theoretically and experimentally, both in the gas phase and in solution [63].

In the case of gas phase reactions e.g. $X^- + CH_3Y \rightarrow Y^- + CH_3X$ a double well profile is present in the Reaction Profile (Fig. 11)

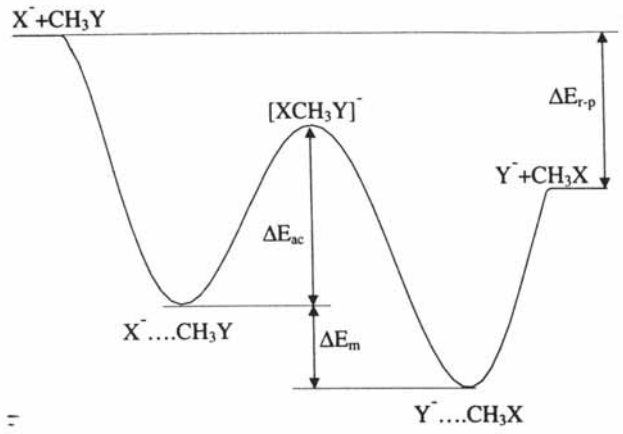

Figure 11. Reaction Profile for a S_N2 reaction in the gas phase (Reprinted with permission by the American Chemical Society - Reference [64]).

We tried to interpret the reaction pathway via DFT based concepts (η, S …) and principles (HSAB, MHP), using a variety of X, Y combinations [64]. 6-31+G* optimized structures were generated for reactants, products, transition states (TS) and ion-molecule complexes. A remarkable correlation is found between ΔE_m both with the calculated $\Delta E_{p\text{-}r}$ (r^2=0.97) and the experimental heat of reaction (r^2=0.99) indicating the relevance of ΔE_m. This quantity shows, e.g. in the case of the $X^- + CH_3F \rightarrow CH_3X + F^-$ reaction, a remarkable correlation with the difference in hardness between F and the group X (Figure 12). The hard F atom in CH_3F can be expected also to harden its neighborhood, *in casu* the carbon atom thereby favoring an interaction with a harder X^- according to the HSAB principle. One thereby regains Pearson's statement about S_N2 reactions that "when nucleophile and leaving group have similar hardnesses, reaction rates are relatively high".

Gazquez [65] developed a formalism to relate the reaction energy and the activation energy to differences in hardness between reagents, products and TS. He showed that $\Delta E_{p\text{-}r}$ should be proportional to $\frac{1}{\Sigma S_r} - \frac{1}{\Sigma S_p}$ where ΣS_r and ΣS_p denote the softness sum for reactants and products, respectively

$$\Delta E_{p-r} \sim \frac{1}{\Sigma S_r} - \frac{1}{\Sigma S_p} \tag{15}$$

It is clearly seen that an exothermic reaction yields

$$\Sigma S_r > \Sigma S_p \tag{16}$$

i.e. products which are harder than reagents, thus recovering the MHP. It should however be remarked that the stringent conditions to be satisfied in the proof of the MHP (constancy of both the external and chemical potential) put severe restrictions on situations in which the principle is applied. For a recent detailed discussion we refer to Chandra and Uchimaru [67]. When applying (15) to the ion-reagent and product complexes one expects a relationship

$$\Delta E_m \approx \frac{1}{S_{\substack{\text{prod}\\\text{complex}}}} - \frac{1}{S_{\substack{\text{reag}\\\text{complex}}}} \sim \frac{1}{\alpha_{\substack{\text{prod}\\\text{complex}}}} - \frac{1}{\alpha_{\substack{\text{reag}\\\text{complex}}}} \approx \Delta E_{r,\alpha} \tag{17}$$

where the proportionality between softness and polarizability (α) [66] has been exploited. In Fig. 11 we observe that $\Delta E_{r,\alpha}$ is always negative (evolution from a complex with lower hardness to one with higher hardness) and that ΔE_m correlates with $\Delta E_{r,\alpha}$ (separate correlations for hard and soft R groups have been drawn).

Turning now to kinetic aspects the central barrier can be regarded as providing the activation energy ΔE_{ac}. Adopting a similar ansatz as before in eq. (17) we looked for two correlations between ΔE_{ac} and the difference $\frac{1}{\alpha} - \frac{1}{\alpha_{TS}}$. Again two correlations can be drawn, one for soft groups, one for hard groups as seen in Fig. 14.

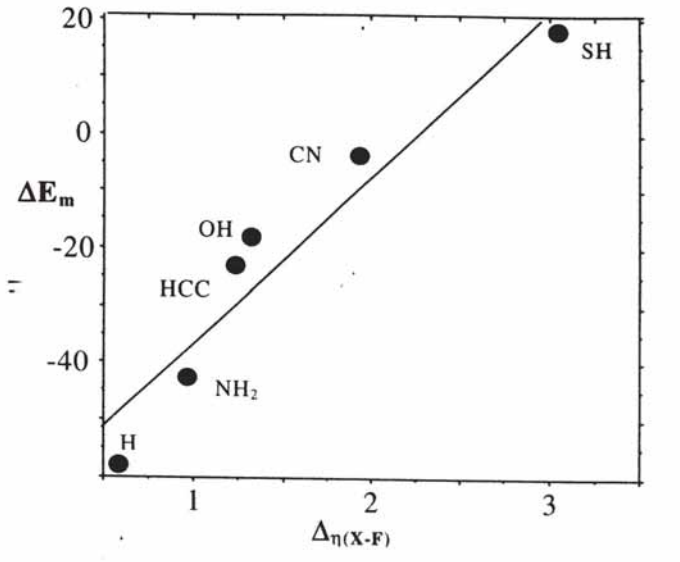

Figure 12. Calculated reaction energy ΔE_m (in kcal mol^{-1}) as a function of the group hardness difference between the X group and fluorine, $\Delta\eta_{X\text{-}F}$ (Reprinted by permission by the American Chemical Society - Reference [64]).

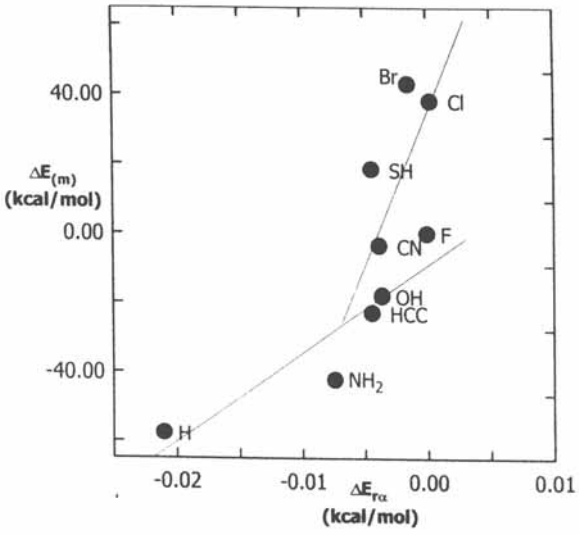

Figure 13. Calculated reaction energy ΔE_m (in kcal mol^{-1}) as a function of the reaction energy $\Delta E_{r,\alpha}$ (in a.u.) obtained via the Gazquez approach. Separate linear correlations for hard (X = H, NH_2, OH, F) and soft (X = HCC, CN, SH, Cl) nucleophiles are shown (Reprinted by permission by the American Chemical Society - Reference [64]).

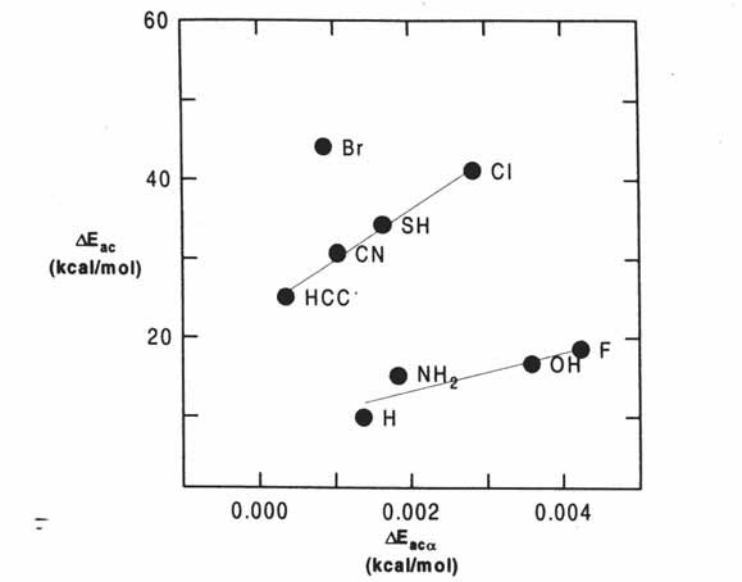

Figure 14. Calculated values of the central barrier energies ΔE_{ac} (kcal mol^{-1}) as a function of the central barrier $\Delta E_{ac,\alpha}$ value (in a.u.) obtained via the Gazquez approach. Separate linear correlations for hard and soft nucleophiles are shown as in Figure 12. (Reprinted by permission by the American Chemical Society - Reference [64]).

These recent results show that the use of DFT based concepts such as softness might shed further light on the reactivity within the context of both the HSAB and MHP principles.
In the next paragraph the HSAB principle is further exploited in the study of regioselectivity in organic reactions.

2.2.3. Regioselectivity in organic reactions: the HSAB principle

As stated above the HSAB principle has been given theoretical support by Parr and Pearson, later on by Gázquez. Based on the global properties of the reacting systems (acid (A) and base (B)) with global softness values S_A and S_B it was shown, based among others on the idea of equalization of electronic chemical potentials (cf. §1.3.2), that the largest interaction energy for constant S_A occurs when S_B equals S_A thereby regaining the HSAB principle [68] . If the interaction sites in A and B are specified (say k in A and l in B) it was shown by Gazquez and the present author [68] that the demand

$$S_A = S_B \qquad (18a)$$

is converted into an analogous equation at local level , i.e.

$$s_{A,k} = s_{B,l} \qquad (18b)$$

where $s_{A,k}$ and $s_{B,l}$ are the local softness values at sites k and l.

Obviously this expression is ready for use in the study of regioselectivity problems. As an example (for further applications see [69]) we briefly discuss the regioselectivity of Diels Alder reactions using the softness matching (18b) approach in at local level [68b].

The predominance of orthoregioisomers in the cycloaddition of 1-substituted dienes **1** and asymmetrical dienophiles **2**

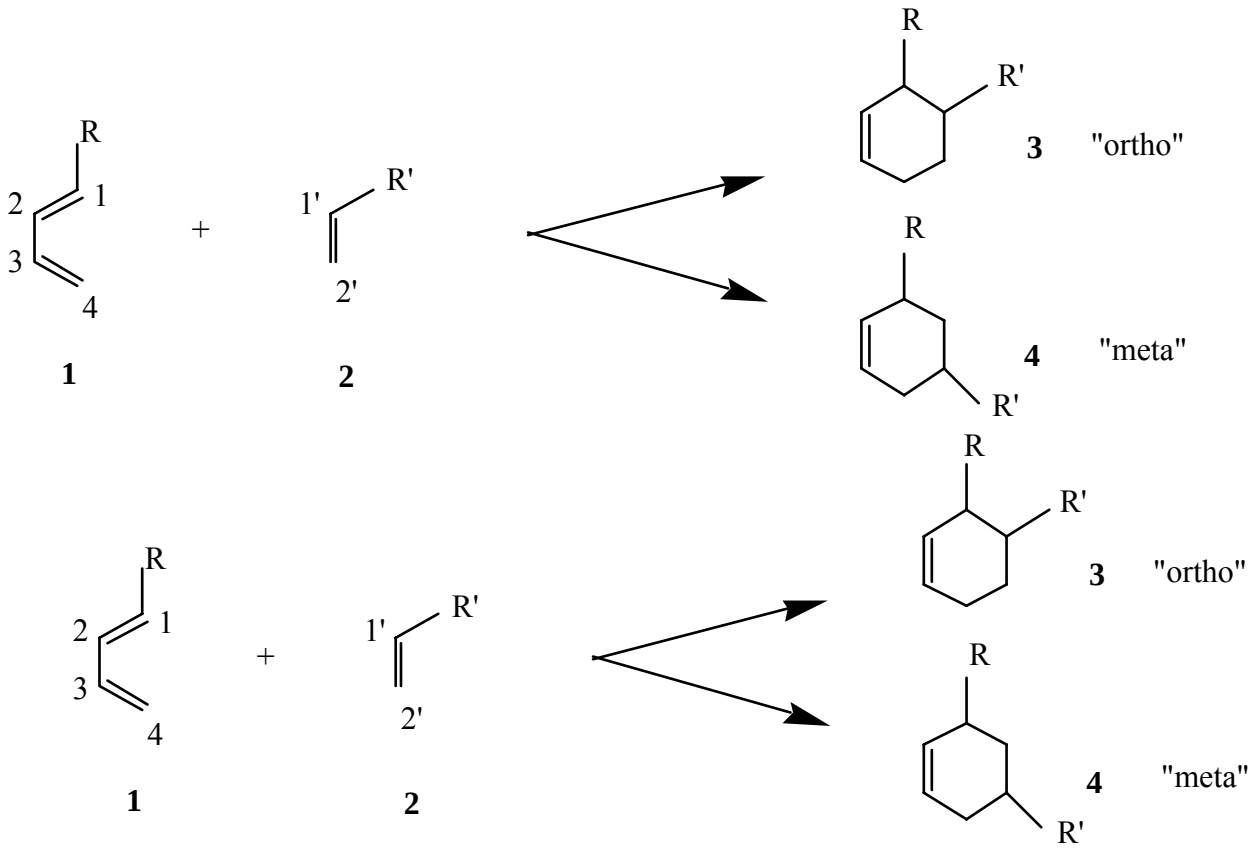

cannot be explained by electronic effects, as replacement of an electron donating substituent by an electron-attracting one does not alter the regioselectivity as discussed by Anh and coworkers [70].

In the double local-local approach of the HSAB principle we considered the local softness resemblance of the termini combinations 1 and 1', 4 and 2', as compared to the 1-2', 4-1' ones. The latter combination yields the meta product, the former the paracycloadduct, considered (cf sterical hindrance) as the contrathermodynamic reaction product.

In the cases R=-Me, -OMe, -COOH, -CN, $-NH_3$, $-NMe_2$, $-NEt_2$, and -OEt and R' = -COOH, -COOMe, -CN, -CHO, $-NO_2$ and -COMe (ensuring in most cases a Normal Electronic Demand reaction type, the dienophile being the electrophilic partner and the diene the nucleophilic one), we calculated local softness values s_1^-, s_1^+, s_2^+, and s_4^- from 3-21G optimized structures at the same level*.

In order to look for a simultaneous fulfillment of the local HSAB principle at both termini the following local softness similarly indicators were evaluated.

* The subscripts (-) and (+) stand for softness vs. electrophilic and nucleophilic attacks respectively.

$$S_{ortho} = \left(s_1^- - s_{1'}^+\right)^2 + \left(s_4^- - s_{2'}^+\right)^2$$
$$S_{meta} = \left(s_1^- - s_{2'}^+\right)^2 + \left(s_4^- - s_{1'}^+\right)^2 \quad (19)$$

Upon analysis of the Frontier Molecular Orbital-energies, the diene could always be identified as the electron donating system and the dienophile acting as electron acceptor.

It is seen that in the 8×6=48 cases studied, corresponding to all R and R' combinations, S_{ortho} is always smaller than S_{meta} except when a CN substituent is present either in the diene or the dienophile. However the DFT related reactivity parameter for the CN group was shown to be highly sensitive to correlation effects. Moreover the idea when writing down equations (19) is based on the hypothesis of a reaction with both couples of termini reacting at the same rate (synchronicity). Concertedness however is not a synonym to synchronicity prompting us to look for the smallest of the four quadratic forms in (19) which in almost all cases turns out to be the $(s_4^- - s_{2'}^+)^2$ term.

This result points into the direction of the C_4-$C_{2'}$, bond forming faster than the C_1-$C_{1'}$ bond, in obvious agreement with the demand of equal softness of interacting termini as there are most remote from R and R'. The asynchronicity in the mechanism suggested on this basis is confirmed by Houk's transition state calculations [71] where in all cases with R and R'≠H asymmetric transition states were found with the C_4-$C_{2'}$ distance being invariably shorter than C_1-$C_{1'}$. This HSAB study performed at the local-local level provides an answer to Anh's long pending hypothesis [70] stating that "it is likely that the first bond would link the softest centers". Important work broadening the scope of this type of approach has been delivered in recent years among others by Nguyen and coworkers, partly in collaboration with the authors, including free radical additions to olefins [72], hydration of cumulenes [73], 2+1 cycloadditions between isocyanide and heteronuclear dipolarophiles [74], cycloaddition reactions between a 1,3-dipole and a dipolarophile [75] and excited state [2+2] photocycloaddition reactions of carbonyls [76]. On the other hand Ponti [77] presented a generalization of the ansatz via eqn (19).

2.2.4. Similarity in Reactivity

Similarity in a fundamental concept in chemistry and pharmacology. In the design of drugs for example one supposes that molecules with similar structures will also exhibit similar biological or physiological activities [78]. The rapid development of computational techniques in recent years has enabled a systematic investigation of the similarity concept suited for quantitative studies of molecular activity [79]. Several similarity indices have been proposed among which the Carbo Quantum Molecular Similarity Index Z_{AB} has played a prominent role [80]. In simplest form it can be written as

$$Z^{\rho}_{AB} = \frac{\int \rho_A(\underline{r})\rho_B(\underline{r})d\underline{r}}{\left[\int \rho_A^2(\underline{r})d\underline{r} \bullet \int \rho_B^2(\underline{r})d\underline{r}\right]^{1/2}} \quad (20)$$

or introducing the shape factor $\sigma(\underline{r})$ [81]

$$\rho(\underline{r}) = \sigma(\underline{r})N$$

$$Z^{\rho}_{AB} = \frac{\int \sigma_A(\underline{r})\sigma_B(\underline{r})d\underline{r}}{\left[\int \sigma_A^2(\underline{r})d\underline{r} \bullet \int \sigma_B^2(\underline{r})d\underline{r}\right]^{1/2}} \quad (21)$$

indicating that the similarity index only depends on the shape of the density distribution and not on its extent. To obtain a more reactivity related similarity index we proposed to replace the electron density in eq. (21) by the local softness $s(\underline{r})$ (cf. § 1.3.2.) [82] yielding the following expression

$$Z^{s}_{AB} = \frac{\int f_A(\underline{r})f_B(\underline{r})d\underline{r}}{\left[\int f_A^2(\underline{r})d\underline{r} \int f_B^2(\underline{r})d\underline{r}\right]^{1/2}} \quad (22)$$

where the local softness has been filtered out.

The index (22) has been tested via similarity analysis of peptide isosteres first using the Carbo and Hodgkin Richards indices [82a]. In the field of peptidomimetics analogues of the peptide bond [83] are looked for, showing however resistance to nucleophilic attack. Functional groups proposed in the vast literature in this domain are CH=CH, CF-CH, CH_2-CH_2, CH_2-S, $COCH_2$, CH_2-NH etc. We tested the similarity of a model system CH_3-CO-NH-CH_3 with its analogues on the basis of the similarity indices involving ρ (20) and s (22). DFT has been used here also as a computational tool using the B3PW91 exchange correlation potential [19a] [84] combined with a 6-311G* basis set [8b]. Table 2 shows that the sequences for Z^{ρ} and Z^{s} are not identical. The highest density similarity is observed for trans-butene, which is not unexpected in view of the trans structure of the peptide bond and the resulting matching of the terminal chains. However, turning to the softness similarity, the Z fluorinated alkene structure shows higher resemblance with the amide bond due to the similarity in polarity with the carboxyl group. The potential use of C=C-F as a peptidomimetric is in accordance with the results of [85].

Notice that the softness similarity has been calculated on the basis of an average of $s^{+}(\underline{r})$ and $s^{-}(\underline{r})$. The high similarity index thus represents a similarity in an average interaction of the model system, including terminating groups, with the surroundings, whereas (not shown) the similarity for a nucleophilic attack is very low (0.016 for the Z^{s+}_{AB} index) [82]. Summarizing, a combined search for optimal Z^{ρ}_{AB} (identical shape) - if necessary with a different type of index, such as Hodgkin's one [82][86] including extent - and optimal Z^{s}_{AB} might be a valuable approach not only in this case but in rational drug design as a whole. In a more recent study [82b] one of the remaining problems in this approach, the orientational and translational dependence of Z, was avoided by introducing the concept of an autocorrelation function of the property considered.

Table 2 : Similarity indices Z^{ρ}_{AB} and Z^{s}_{AB} for peptide isosteres of CH_3-CO-NH-CH_3 (B3PW91/ 6-311G* calculation). The centers of the central bond were brought to coincidence.

- CO-NH -	Z^{ρ}_{AB}	Z^{s}_{AB}
- CH=CH - (trans)	0.582	0.576
- CH=CH - (cis)	0.506	0.501
- CF=CH - (Z)	0.418	0.635
- CH_2-CH_2 -	0.466	0.495
- CH_2-S -	0.034	0.337
- CO-CH_2 -	0.531	0.108
- CH_2-NH -	0.412	0.559

2.3. Inorganic Chemistry: Zeolites

Zeolites are alumino-silicates consisting of SiO_4 and AlO_4 tetrahedra linked to each other by their corner oxygens. The alumino silicate structure is negatively charged due to the isomorphic subsitution of silicon by aluminum [87]. This negative charge is balanced by exchangeable cations.

When protons are introduced as counterions, the zeolite becomes a Brϕnsted acid, the protons being positioned on an oxygen atom connecting an aluminum and a silicon atom. These bridging hydroxyls [88] are at the origin of the acid catalysis application of zeolites [89]. Another aspect of the structure of zeolites is the occurrence of large vacant interconnected spaces forming long, wide channels of varying size depending on the type considered allowing the crystal to act as a molecular sieve [90].

For many years [91] the concepts of electronegativity, softness, hardness …. were exploited by us in the study of the acidity of bridging hydroxyl in zeolites, of utmost importance in their catalytic properties (for a review see [92]).

Due to space limitations and because some fundamental aspects of this kind of study are already present in § 2.2.1. on the acidity of alcohols, we concentrate in this paragraph on a recently aborded topic especially highlighting the possibilities of Computational Chemistry, switching at the end however again to Conceptual DFT : adsorption in zeolites.

The problem we recently addressed [93, 94, 95] was the selectivity of adsorption of gases [96] for which up to now no parameter free ab initio quantum chemical studies were performed yet [90]. Below we summarize the results for the interaction of small molecules (such as N_2, O_2, CO), with a NaY faujasite type zeolite, more specifically with the α cage.

At sufficiently low pressure adsorption is governed by Henry's law [96]

$$q = Kp \tag{23}$$

where q is the amount of substance per unit volume in the adsorbed phase and p the pressure. Henry's constant K can be written as [97]

$$K = \frac{BI}{aRT} \tag{24}$$

where B is the number of cavities in which adsorption can take place per unit mass of zeolite. The quantity "a" equals 1 for a monoatomic gas, 4π for a linear molecule and $8\pi^2$ for a non linear molecule. The configuration integral I is defined as

$$I = \int e^{-E(\underline{r},\underline{\Phi})/RT} d\underline{r}d\underline{\Phi} \tag{25}$$

where E represents the interaction energy of the adsorbing molecule with the zeolite cage at position $\underline{r}$ and with orientation $\underline{\Phi}$. The integration is performed over the volume V of the supercage.

The cluster representing the supercage and its nearest environment was chosen to be "as large as possible" (within computational limits) and with an Si/Al ratio of 3. The 232 atoms cluster, involving OH groups as terminators is shown in Figure 15, where also four cationic adsorption sites of type II, the ones "active" in the conditions that we consider are present, one of them being indicated.

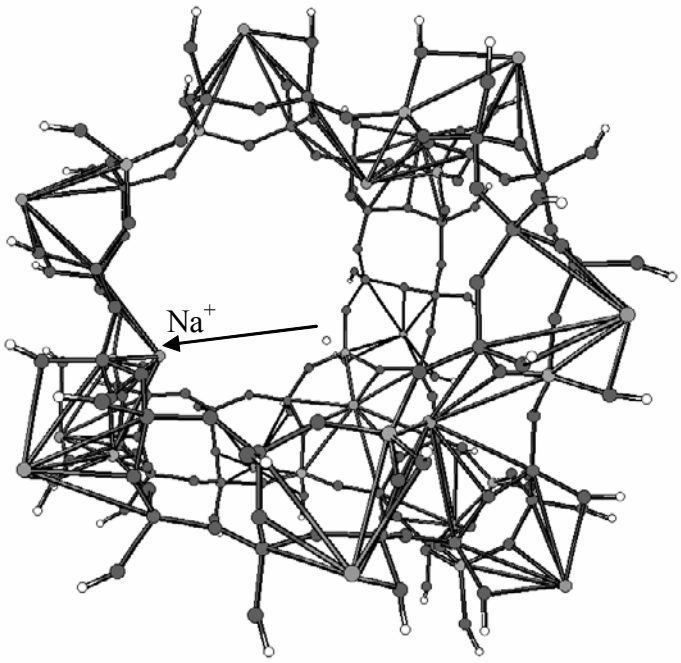

Figure 15 : Cluster used to model the large cage of faujasite Y (Reprinted with permission by J. Wiley - Reference [94])

An embedded cluster method was then adopted, considering the molecule in the field generated by the cage atom charges, the latter being obtained in a single run at Hartree Fock STO-3G or 3-21G level. The points at which the interaction energy is evaluated are selected by constructing a cubic grid with a grid distance of 0.50 Å in each direction and considering the center of each cube generated in this way. The expression (25) is thereby approximated as

$$I \approx \frac{4\pi}{3} \sum_i \left(e^{-E_{x,i}/RT} + e^{-E_{y,i}/RT} + e^{-E_{z,i}/RT} \right) \Delta V_i \qquad (26)$$

where the three terms account for three mutually perpendicular orientations of the molecule, each one given an equal weight to simplify the orientational integration $d\underline{\Phi}$. ΔV_i equals 0.125 Å^3.

A supplementary condition was introduced imposing a minimal distance between an atom of the adsorbing molecule and a cage atom (cf. the treatment of the repulsive term in the potential, for details see [94]). At these small distances E becomes positive and its contribution to I, via the exponential function, very small. This procedure leads to the consideration of not less than ± 3000 cage-points necessitating an in-depth search for an optimal quality/cost ratio in the procedure for the interaction energy evaluation. The optimal procedure, from a quality/cost ratio point of view, turned out the following one [94,95,98]. The starting point was the energy expansion of a molecule in a non-uniform electric field [99].

$$\begin{aligned} E(F_\alpha, F_{\alpha\beta}, F_{\alpha\beta\gamma}, ...) = E - \mu_\alpha F_\alpha - \frac{1}{3}\Theta_{\alpha\beta}F_{\alpha\beta} - \frac{1}{15}\Omega_{\alpha\beta\gamma}F_{\alpha\beta\gamma} \\ - \frac{1}{105}\Phi_{\alpha\beta\gamma\delta}F_{\alpha\beta\gamma\delta} - \frac{1}{2}\alpha_\alpha F_\alpha F_\beta - \frac{1}{6}\beta_{\alpha\beta\gamma}F_\alpha F_\beta F_\gamma \end{aligned} \qquad (27)$$

where F_α, $F_{\alpha\beta}$, ...represent the field, field gradient, ... components whereas μ_α, $\Theta_{\alpha\beta}$, $\Omega_{\alpha\beta\gamma}$,… stand for the dipole, quadrupole, octadecapole, … components and α_α, $\beta_{\alpha\beta}$, … are the dipole polarizability and the first hyperpolarizability. In the case of a neutral molecule of the $C_{\infty,v}$ type (CO) the expression simplifies to (the molecular axis is taken to be the z-axis)

$$\begin{aligned} E(q, R, \theta) = E^o + \sum_i \mu_z q_i R_i^{-2} \cos\theta_i + \sum_i \Theta_{zz} q_i R_i^{-3} (3\cos^2\theta_i - 1)/2 \\ + \sum_i \Omega_{zzz} q_i R_i^{-4} (5\cos^3\theta_i - 3\cos\theta_i)/2 \\ + \sum_i \Phi_{zzzz} q_i R_i^{-5} (35\cos^4\theta_i - 30\cos^2\theta_i + 3)/8 \\ - \sum_i \underline{F}_i^2 (\alpha_{zz}\cos^2\theta_i + \alpha_{xx}\sin^2\theta_i)/2 \end{aligned} \qquad (28)$$

$\underline{F}_i$ represents the electric field at the origin of the molecule due to the surrounding point charges. In $D_{\infty,h}$ cases (N_2, O_2, CO_2, …) terms in μ and Ω vanish.

The quality of this approach in dependent on the number of terms retained in the expressions (27) and (28) and the quality of the multi-pole moments, polarizabilities … These were calculated with DFT methodology (B3LYP functional [19]) combined with Dunning's extremely large basis sets (the augmented -correlation consistent and polarized - valence - quadruple or quintuple basis sets (AVQZ or AV5Z) [100][101]).

This methodology was proved by us to yield multipole moments which are in excellent agreement with experiment [98] [102].

In Table 3 the main results are summarized for N_2, O_2, CO, CO_2, C_2H_2. Besides Henry constants, also separation constants α (ratio of two Henry constants) and the isosteric heats of adsorption are tabulated. The latter values were obtained via the Van't Hoff equation

$$\frac{\partial \ln K}{\partial \left(1/T\right)} = -\frac{\Delta H^o}{R} \tag{29}$$

for which K was calculated in the temperature interval between 260 and 340K with an increment of 10K and using a linear regression.

Table 3: Henry constants, separation constants and isosteric heats of adsorption on NaY : comparison between theory and experiment [94][98].

	N_2	O_2	CO	CO_2	C_2H_2
K	3.320	1.830	9.951	63.33	196.8
K_{exp}	31.4	15.4	85		
$\Delta H°$	-12.9	-7.9	-18	-27	-29
ΔH_{exp}	-14	-9.4	-20	-37	

	N_2/O_2	CO/N_2	CO_2/CO
α	1.81	2.99	6.36
α_{exp}	2.04	2.70	

As a whole these results yield K values which are systematically one order of magnitude too small but showing correct sequences. The order of magnitude should be considered within the correct context : a uniform underestimation of the interaction energy of only 1.4 kcal mol^{-1} already yields an order of magnitude underestimation of K. This extremely high sensitivity is of course due to the sensitivity of the potential in the repulsion part, plugged into an exponential in the configuration integral. The ratio K_{exp}/K is almost constant with values of 9.45, 8.41, 8.54 respectively. As a consequence the separation constants are in excellent agreement with experiment. The isosteric heats of adsorption also show very good agreement in absolute value and reproduce the experimental sequence. In our opinion these investigations pave the way for future studies involving more complex molecules where the lines drawn here, together with increasing computer hard and software and DFT based methodology, may finally yield to calculations which will be of great use in the design of zeolites for well defined purposes (e.g. gas separation).

An alternative for the interaction energy evaluation including electrostatic and polarization effects was proposed in a conceptual DFT context. Using a DFT perturbational approach we obtained the following expression for the interaction energy

$$\Delta E = \sum_i q_i V(\underline{R}_i) + S\sum_i\sum_j q_i q_j \left(\int \frac{f(\underline{r})}{|\underline{r} - \underline{R}_i|} d\underline{r} \int \frac{f(\underline{r}')}{|\underline{r}' - \underline{R}_j|} d\underline{r}' \right) - \int \frac{f(\underline{r})}{|\underline{r} - \underline{R}_i||\underline{r} - \underline{R}_j|} d\underline{r} \tag{30}$$

The first term corresponds to the electrostatic interaction $V(\underline{R}_i)$ as given by the molecular electrostatic potential at position $\underline{R}_i$ where charge q_i is located, multiplied by this charge. The second term is the polarization term [103] in which both the total softness, S, and the fukui function, $f(\underline{r})$, appear. Further work to evaluate in an efficient way the integral in the second term is in progress, the basic requirements for the evaluation of the interaction energy being the molecular electrostatic potential and fukui function ($V(\underline{r})$ and $f(\underline{r})$) and the total softness nowadays ready available at a high precision level.

Conceptual DFT can thus be exploited in the study of adsorption behaviour of zeolites, as also especially witnessed in the work by Chatterjee and coworkers using the condensed Fukui function and local softness to estimate and rationalize the interaction energy of several small molecules with a zeolitic framework [104-106]. An attempt was made to explain selective permeation of these molecules [105] and the choice of the best template for a particular zeolite synthesis by estimating the reactivity of the templating molecule [106].

2.4. Biochemistry : Influence of point mutations on the catalytic activity of subtilisin

As an example of our work in biochemistry we summarize very briefly recent studies in which the embedded cluster approach presented in § 2.3 was used to study the active sites in enzymes, more precisely the catalytic triad in subtilisin [107] and Ribonuclease T_1 [108].

The methodology followed in these studies shows similarities with part of the zeolite adsorption studies (high level quantum chemical calculation on that part of the system at which the active site is situated and a point charge environment for the residues farther away). The results of the subtilisin study are given as an example.

Subtilisin is a bacterial enzyme belonging to the class of the serine proteases characterized by a catalytical apparatus consisting of three amino acid residues, serine, histidine and aspartate : the catalytic triad (Asp32 - His64 - Ser221 for subtilisin) (Fig. 16). In the rate determining step of the hydrolysis reaction (see Fig. 17) the hydroxyl proton of Ser221 is transferred to the $N_{\varepsilon 2}$ atom of His64. Simultaneously a nucleophilic attack by the hydroxyl oxygen of Ser221 at the carbon atom of the scissile peptide bond occurs. The role of the aspartate residue is to enhance the nucleophilicity of Ser221 due to the electric field of the charged aspartate side chain and to provide electrostatic stabilization of the tetrahedral intermediate.

The role of the catalytic triad amino acids was studied by Carter and Wells : both single and double alanine substitutions of these residues led to a lowering of the catalytic rate constant k_{cat} [109]. Russell and Fersht studied the effect on k_{cat} for mutations occurring outside the catalytic triad [110].

These effects were studied by placing the catalytic triad into an environment of ChelpG point charges representing all atoms of the amino acids within a 15 Å sphere around His64, and obtained from ab initio calculations on isolated amino acids; the structural data on the wild type enzyme were taken from X-ray diffraction studies [111], mutations were carried out *in computero*. The

nucleophilicity of the Ser221 oxygen was investigated using local softness and (models for) the local hardness : the charge on the oxygen atom and the MEP.

Local softness turned out to be not successful when correlating s_O^- with k_{cat} values in line with Fersht's statement that the nucleophilic attack of the serine on the substrate can be considered as an attack on a hard nucleophilic center [112]. We now further concentrate on local hardness descriptors. When comparing the wild type enzyme and the His64 Ala mutant with, respectively, the Asp32 Ala and Asp32 Ala : His64 Ala mutants, Table 4 shows a less negative charge and, much more pronounced, a less negative MEP value, indicating that the interaction of the catalytic serine with an electrophile is less advantageous in the aspartate mutants. These results are in agreement with experiments pointing out an enhancement of the serine nucleophlicity by the aspartate residue [113].

Table 4 : Serine oxygen charge (q_O) (au) and MEP minimum around this oxygen atom ($V(\underline{R})_{min}$) (in $kcalmol^{-1}$) calculated for the wild-type and mutant enzymes (3-21G Hartree Fock with ChelpG charges).

	q_O	$V(\underline{R})_{Min}$
Wild Type	-0.7719	-121.72
Asp32 Ala	-0.7440	-75.64
His64 Ala	-0.7665	-113.13
Asp32 Ala : His64 Ala	-0.7487	-67.92

A more quantitative picture is obtained when studying the atomic charges and MEP vs. the experimental k_{cat} values [109] for the enzymes when the mutations were performed in the environment of the catalytic triad (Table 5). A correlation coefficient of 0.927 was obtained in the case of the charges (Figure 18).

Table 5 : Experimental k_{cat} values (s^{-1}) and calculated charges q_O (au) and MEP minimum $V(\underline{R})_{min}$ ($kcal\ mol^{-1}$) for the serine oxygen for wild-type, aspartate 99 and glutamate 156 mutant enzymes.

	k_{cat}	q_O	$V(\underline{R})_{min}$
1. Wild Type	57	-0.7719	-121.72
2. Asp99 Ser	45	-0.7610	-121.33
3. Asp99 Lys	30	-0.7581	-121.30
4. Glu156 Ser	55	-0.7700	-122.96
5. Glu156 Lys	79	-0.7748	-124.57

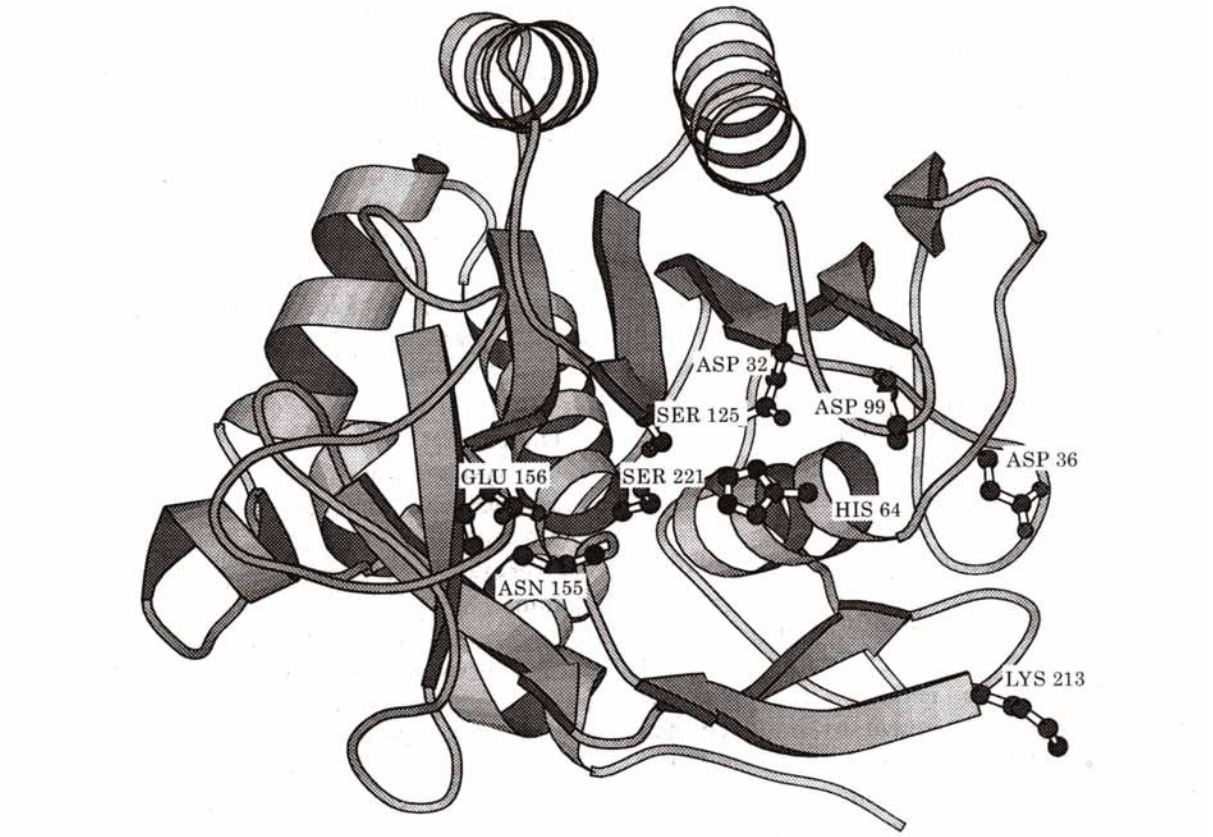

Figure 16. Schematic drawing of subtilisin. Side chains of the residues of importance in the discussion are shown explicitely (Reprinted with permission by Academic Press, Reference [107]).

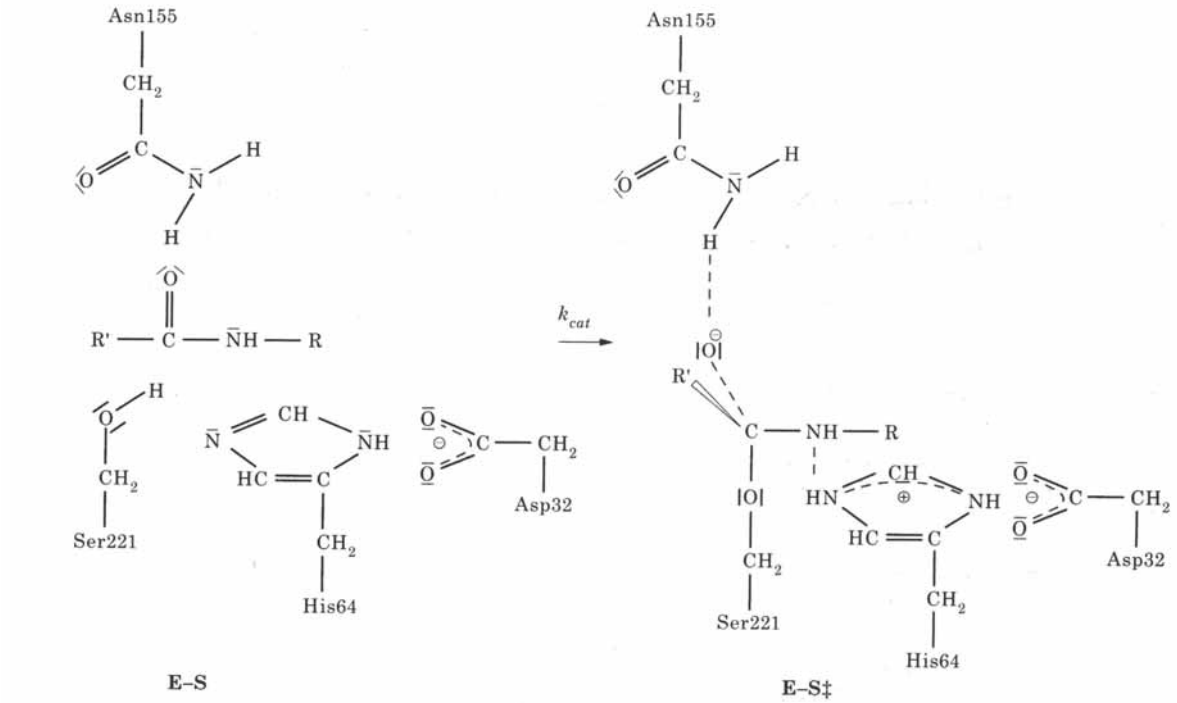

Figure 17. Schematic representation of the enzymatic reaction of serine proteases; E-S is the enzyme substrate complex, E-S$^{\neq}$ the tetrahedral reaction intermediate (Reprinted with permission by Academic Press - Reference [107])

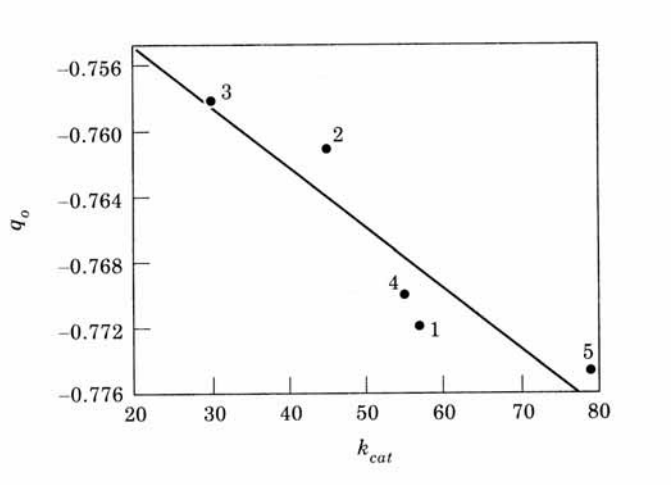

Figure 18. Atomic charge on the serine oxygen atom q_0 vs. experimental k_{cat} (see Table 5).

3. Conclusions

In this contribution it is seen that Quantum Mechanics gave birth to new branches in chemistry, Quantum Chemistry and Computational Chemistry, which nowadays provide the theoretical/conceptual and computational framework for studying "real" chemical problems, i.e. systems whose size promotes them to valuable models for the actual reaction partners, their environment, and their interactions. Within this context Density Functional is a source of increasing importance both for concepts and computational techniques.

Application to reactivity problems (considered within a broad context including kinetic as well as thermodynamic aspects) in organic, inorganic and biochemistry shows that present day quantum chemistry becomes a priceless tool to compute and understand phenomena in various traditional subfields of chemistry. Especially the DFT ansatz provides an ideal situation to bridge the gap between chemistry and physics in the years to come [114].

4. Acknowledgements

Besides his coauthor PG wants to thank his past and present Ph.D. students and postdoctoral associates W. Langenaeker, A. Baeten, K. Choho, B. Safi, G. Boon, S. Damoun, F. Tielens, whose work was summarized in this contribution. Special thanks to Professor F. Mendez (Mexico) for the collaboration on organic reactivity during his stay in Brussels, to Professors W. Mortier (Exxon-Mobil-KU Leuven), R. Schoonheydt (KU Leuven) and G. Baron (VUB) for the longstanding collaboration on zeolites and Professors L. Wyns and J. Steyaert (VUB) for backing the quantum biochemical research.

5. References

1. Dirac, P.A.M. *Proc. Roy.Soc.(London)*, **1929**,*123*, 714.
2. Heitler, W.; London, F. *Z. Phys.* **1927**,*44*, 455.
3. Pauling,L. *The Nature of the Chemical Bond*, Third Edition, Cornell University Press, Ithaca, 1960.
4. For a classic and authoritative account of Hückel's approach and its applications see A. Streitwieser, A. *Molecular Orbital Theory for Organic Chemistry*; John Wiley, 1961.
5. Mc Weeny, R. *Coulson's Valence*; Third Edition, Oxford, 1979.
6. (a) Hund, F. *Z. Phys*., **1928**, *51*, 759.
   (b) Mulliken, R. S. *Phys Rev.*, **1928**, *32*, 186.
7. Roothaan, C. C. J. *Rev. Mod. Phys*., **1951**, *23*, 69.
8. (a) For an overview see Hartree, D.R. *The Calculation of Atomic Structures*, John Wiley, New York, 1957.
   (b) Hehre, W. J.; Radom, L.; Schleyer ,P. v. R.; Pople, J. A. *Ab Initio Molecular Orbital Theory*, Wiley, New York, 1986.
9. Møller, C.; Plesset, M.S. *Phys. Rev.* **1934**, *46*, 618.
10. Shavitt, I. *The Method of Configuration Interaction in Modern Theoretical Chemistry*, Vol.3, Methods of Electronic Structure Theory, H.F.Schaefer III Editor, Plenum Press, New York, 1977, p.189.
11. Bartlett, R.J. *J. Phys. Chem.*, **1989**, *93*, 1697.
12. Pople, J.A., et al., *GAUSSIAN 98*, **1998**, and previous releases (GAUSSIAN 94, GAUSSIAN 92, ..., GAUSSIAN 70), Gaussian Inc., Pittsburgh A.
13. *The Encyclopedia of Computational Chemistry*, Schleyer P. v. Rague; Allinger, N. L.; Clark,T.; Gasteiger, J.; Kollman, P. A.; Schaefer, H. F.; Schreiner, P. R. (Eds.), John Wiley & Sons Ltd., Chichester 1998.
14. Pople, J.A. *J. Chem. Phys*., **1966**, *43*, S229.
15. Hohenberg,P.; Kohn, W. *Phys. Rev. B* ,**1964**, *136*, 864.
16. Mc Weeny,R.; Sutcliffe, B.T. *Methods of Molecular Quantum Mechanics*, Academic Press, London, 1969, Chapter 4.
17. Kohn W.; Sham, L. *Phys. Rev. A*, **1965**, *140*, 1133.
18. Parr,R.G.; Yang,W. *Ann. Rev. Phys. Chem.*, **1995**, *46*, 701.
19. (a)Becke, A.D. *J. Chem. Phys*, **1993**, *98*, 5648.
   (b) Lee, C.; Yang, W.; Parr, R.G. *Phys. Rev. B*, **1998**, *37*, 785.
20. Geerlings, P.; De Proft,F.; Langenaeker,W. *Adv. Quantum Chem.*, **1999**, *33*, 303.
21. Kohn, W.; Becke, A.; Parr, R.G. *J. Phys. Chem.*, **1996**, *100*, 12974.
22. Koch,W.; Holthausen, M.C. "*A Chemistry's Guide to Density Functional Theory*", Wiley-VCH, Weinheim, 2000.
23. Parr,R.G. in "*Density Functional Methods in Physics*", Dreizler R.M.; da Providencia,J., Editors, Plenum, 1985, p. 141.

24. England, W.; Salmon,L.S.; Rüdenberg,K. *Fortschr. Chem. Forsch.*, **1971**, *23*, 3 and references therein
25. Foster, M.; Boys, S.F. *Rev. Mod. Phys.* **1960**, *32*, 300.
26. Schaftenaar, G.; Noordik, J.H. "*Molden : a pre- and post-processing program for molecular and electronic structures*", *J. Comp.-Aided Mol. Design*, **2000**, *14*, 123.
27. Müller, N.; Pritchard, D.E. *J. Chem. Phys.*, **1959**, *31*, 768.
28. Figeys, H. P.; Geerlings, P.; Raeymaekers, P.; Van Lommen, G.; Defay, N.; *Tetrahedron* , 1975, *31*, 1731.
29. Parr, R.G.; Yang,W. *Density Functional Theory of Atoms and Molecules*, Oxford, 1989, Chapter
30. Parr, R.G.; Donelly, R.A.; Levy, M.; Palke,W.E. *J. Chem. Phys.*,**1978**, *68*, 3801.
31. Iczkowski, R.P.; Margrave, J.L. *J. Am. Chem. Soc.* **1961,** *83*, 3547.
32. Mulliken, R.S. *J. Chem. Phys.*, **1934**, *2*, 782.
33. For a series of papers covering various aspects of electronegativity see : *Structure and Bonding*, Vol.66, Sen, K.D.; Jørgensen, C.K., Editors, Springer Verlag, Berlin, 1987.
34. Nalewajski, R.F.; Parr, R.G. *J. Chem. Phys.* **1982**, *77*, 399.
35. Parr, R.G.; Pearson, R.G. *J. Am. Chem. Soc.*, **1983**, *105*, 7512.
36. Parr, R.G.; Yang,W. *J. Am. Chem. Soc.*, **1984**, *106*, 4049.
37. Fukui, K.; Yonezawa, T.; Shinghu, H. *J. Chem. Phys.* **1952**, *20*, 722.
38. Yang, W.; Parr, R.G. *Proc. Natl. Acad. Sci.*. **1985**, *82*, 6723.
39. Chermette, H. *J. Comp. Chem.*, **1999**, *20* ,129.
40. a) De Proft, F.; Geerlings, P. *Chem. Rev.*, **2001**, *101*, 1451.
    b) Geerlings, P.; De Proft, F.; Langenaeker, W. *Chem. Rev.* , submitted.
41. Sanderson, R.T. *Science*, **1955**, *121*, 207.
42. Sanderson, R.T. *Polar Covalence*, Academic Press, New York, 1983.
43. Pearson, R.G. *J. Am. Chem. Soc.*, **1963**, *85*, 3533.
44. Pearson, R.G. *Chemical Hardness*, J. Wiley, New York, 1997.
45. Chattaraj, P.K.; Lee, P.K.; Parr, R.G. *J. Am. Chem. Soc.*, **1991**, *113*, 1855.
46. Parr, R.G.; Chattaraj, P.K. *J. Am. Chem. Soc.*, **1991**, *113*, 1854.
47. De Proft, F.; Martin, J.M.L.; Geerlings, P. *Chem. Phys. Lett.*, **1996**, *250*, 393; **1996**, *256*, 400.
48. De Proft, F.; Geerlings, P. *J. Chem. Phys.*, **1997**, *106*, 3270.
49. De Oliveira, G.; Martin,J.M.L.; De Proft, F.; Geerlings, P. *Phys. Rev.*, **1999**, *A60*, 1034.
50. See for example the impressive series *The Chemistry of Functional Groups*, Patai, S. Editor, Interscience Publishers, London.
51. De Proft, F.; Langenaeker, W.; Geerlings, P. *J. Phys. Chem.*, **1993**, *97*, 1826.
52. Datta, D.; Nabakishwar, S.S. *J. Phys. Chem.*, **1990**, *94*, 2184.
53. Wray, V.; Ernst, L.; Luna,T.; Jakobsen, H.-J. *J. Magn. Res.*, **1980**,*40*, 55.
54. Pearson, R.G. *J. Am. Chem. Soc.*,**1998**, *110*, 7684.
55. De Proft, F.; Langenaeker,W.; Geerlings, P. *Tetrahedron* , **1995**, *55*, 4021.
56. Lias, S.G.; Bartmess, J.-E.; Liebman, J.F.; Holmes, J.L.; Levin, R.D.; Mallard, W.G. *J. Phys. Chem. Ref. Data*, **1988**, *17* (Suppl 1).

57. Bartmess, J.E.; Scott, J.A.; Mc Iver Jr., R.T. *J. Am. Chem. Soc.*, **1979**, *101*, 6056.
58. Taylor, R. *Electrophilic Aromatic Substitution*, J. Wiley, New York, 1990.
59. Vanermen, G.; Toppet, S.; Van Beylen, M.; Geerlings,P. *J. Chem. Soc., Perkin Transactions 2*, **1986**, 699.
60. Wiberg, K.; Keith, T.A.; Frisch, M.J.; Muacko, M.; *J. Phys. Chem.*, **1995**, *99*, 9072.
61. Safi, B.; Choho, K.; De Proft, F.; Geerlings P. *J. Phys. Chem.*, **1998**, *A102*, 5253.
62. Isaacs, N. *Physical Organic Chemistry*, Longman Scientific and Technical, Singapore, 1995.
63. Shaik, S.S.; Schlegel, H.B.; Wolfe, S. *Theoretical Aspect of Physical Organic Chemistry*, John Wiley, 1992.
64. Safi, B.; Choho, K.; Geerlings, P. *J. Phys. Chem*, , **2001**, *A105*, 591.
65. Gazquez, J.L. *J. Phys. Chem.*, **1997**, *A101*, 8967.
66. Politzer, P. *J. Chem. Phys.*, **1987**, *86*, 1072.
67. Chandra, A. K. ; Uchimaru, T. *J. Phys. Chem. A*, **2001**, *105*, 3578.
68. (a) Gazquez, J.L.; Mendez, F. *J. Phys. Chem.*, **1994**, *98*, 459.
    (b) Damoun, S.; Van de Woude, G.; Mendez, F.; Geerlings, P. *J. Phys. Chem.*,**1997**, *A101*, 886.
69. Geerlings, P.; De Proft, F. *Int. J. Quant. Chem.*, **2000**, *80*, 227.
70. Eisenstein, O.; Lefour, J.M.; Anh, N.T.; Hudson, R.F. *Tetrahedron*, **1977**, *33*, 523.
71. K.N. Houk, K.N.; Li,Y.; Evanseck., J.T. *Angew. Chem. Int. Ed. Engl.*, **1992**, *31*, 682.
72. Chandra, A. K. ; Nguyen, M. T. *J. Chem. Soc. Perkin Trans. 2*, **1997**, 1415.
73. (a) Raspoet, G. ; Nguyen, M. T. ; McGarraghy, M. ; Hegarty, A. F. *J. Org. Chem.*, **1998**, *63*, 6867.
    (b) Nguyen, M. T. ; Raspoet, G. *Can. J. Chem.* **1999**, *77*, 817.
    (c) Nguyen, M. T. ; Raspoet, G. ; Vanquickenborne, L. G. *J. Phys. Org. Chem.*, **2000**, *13*, 46.
74. (a) Chandra, A. K. ; Geerlings, P. ; Nguyen, M. T. *J. Org. Chem.*, **1997**, *62*, 6417 .
    (b) Nguyen, L. T. ; Le, T. N. ; De Proft, F. ; Chandra, A. K. ; Langenaeker, W. ; Nguyen, M. T. ; Geerlings, P. *J. Am. Chem. Soc.*, **1999**, *121*, 5992.
75. (a) Chandra, A. K. ; Nguyen, M. T. *J. Comput. Chem.*, **1998**, *19*, 195.
    (b) Nguyen, L. T. ; De Proft, F. ; Chandra, A. K. ; Uchimaru, T. ; Nguyen, M. T. ; Geerlings, P. *J. Org. Chem.* **2001**, *66*, 6096.
    (c) Le, T. N. ; Nguyen, L. T. ; Chandra, A. K. ; De Proft, F. ; Geerlings, P. ; Nguyen, M. T. *J. Chem. Soc. Perkin Trans. 2* **1999**, 1249.
    (d) Chandra, A. K. ; Uchimaru, T. ; Nguyen, M. T. *J. Chem. Soc. Perkin Trans. 2* **1999**, 2117.
    (e) Chandra, A. K. ; Nguyen, M. T. *J. Phys. Chem. A* **1998**, *102*, 6181.
76. Sengupta, D. ; Chandra, A. K. ; Nguyen, M. T. *J. Org. Chem.* **1997**, *62*, 6404.
77. Ponti, A. *J. Phys. Chem. A* **2000**, *104*, 8843.
78. Rouvray, D.H. *Top. Curr. Chem.*, **1995**, *173*, 2 .
79. Mishra, P.C.; Kumar, A. *Theor. Comput. Chem.*, **1996**, *3*, 257.
80. Carbo, M.; Arnau, M.; Leyda, L. *Int. J. Quant. Chem.,* **1980**, *17*, 1185.
81. Parr, R.G.; Bartolotti, L.J. *J. Phys. Chem.*, **1983**, *87*, 2810.
82. a) Boon, G.; De Proft, F.; Langenaeker,W.; Geerlings, P. *Chem. Phys. Lett.*, **1996**, *295*, 122.

b) Boon, G.; Langenaeker, W.; De Proft, F.; De Winter, H.; Tollenaere, J.P.; Geerlings, P. *J. Phys. Chem.A*, **2001**, *105*, 8805.

83. Spatola, A.F. in *Chemistry and Biochemistry of Amino Acids, Peptides and Proteins*, vol. 7, Weinstein, B. Editor, Marcel Dekker, New York, 1983, p. 267.
84. Perdew,J.P.; Wang, Y.; *Phys. Rev. B*, **1992**, *45*, 13244.
85. (a) Allmendiger, T.; Felder, E.; Hungerbühler, A. *Tetr. Lett.* , **1990**, 7301.
    (b) Bartlett, P.A.; Otake, A. *J. Org. Chem.*, **1995**, *60*, 3107.
86. Hodgkin, E.E.; Richards, W. G. *Int. J. Q. Chem., Quantum Biology Symp.*, **1987**, *14*, 1051.
87. Breck, D.W. *Zeolite Molecular Sieves : Structure, Chemistry and Use*, John Wiley, Canada, 1974.
88. Uytterhoeven, J.B.; Christner, L.G.; Hall, W.K. *J. Phys. Chem.*, **1965**, *69*, 2117.
89. Van Bekkum, H.; Flanigen, E.M.; Jansen, J.C. *Introduction to Zeolite Science and Practice*, Elsevier, Amsterdam, 1991.
90. Sherman, J.D.; *Proc. Natl. Acad. Sci. USA,* **1999**, *96*, 3471.
91. Van Genechten, K.; Mortier, W.J.; Geerlings, P. *J. Chem. Phys.* , **1987**, *86*, 5063.
92. Langenaeker, W.; De Proft,F.; Geerlings, P. *Recent Developments in Physical Chemistry*, Vol. 2, Transworld Research Network, Triviandum, India, 1998,1219.
93. Peirs, J.C.; De Proft, F.; Baron, G.; Van Alsenoy, C.; Geerlings, P. *Chem. Comm.*, **1997**, 531.
94. Tielens, F.; Langenaeker, W.; Ocakoglu, A. R.; Geerlings, P. *J. Comp. Chem.*, **2000**, *21*, 909.
95. Tielens, F. ; Geerlings, P. *J. Mol. Catal.*, **2001**, *A166*, 175.
96. Ruthven, D. M. *Principles of Adsorption and Adsorption Processes*, John Wiley, Canada, 1984.
97. Kiselev, A. V. *Pure Appl. Chem.*, **1980**, *52*, 2161.
98. (a) Tielens, F.; Geerlings, P. *Int. J. Quant. Chem.* **2001**, *84*, 58.
    (b) Tielens, F. ; Geerlings, P. *Chem. Phys. Lett.* **2002**, *354*, 474.
99. Buckingham, A.D. in *Intermolecular Interactions*, Pullman, B. Editor, Wiley, 1988.
100. Dunning Jr., T.H. *J. Chem. Phys.*, **1989**, *90*, 1007.
101. Kendall, R.A.; Dunning Jr., T.H.; Harrison, R.J. *J. Chem. Phys.*, **1992**, *96*, 6796.
102. De Proft, F.; Tielens, F.; Geerlings, P. *J. Mol. Struct. (Theochem)*, **2000**, *506*, 1.
103. Langenaeker, W.; De Proft, F.; Tielens, F.; Geerlings, P. *Chem. Phys. Lett.*, **1998**, *288*, 628.
104. Chatterjee, A. ; Iwasaki, T. ; Ebina, T. *J. Phys. Chem. A* **1999**, *103*, 2489.
105. Chatterjee, A. ; Iwasaki, T. *J. Phys. Chem. A* **1999**, *103*, 9857.
106. Chatterjee, A. ; Iwasaki, T. *J. Phys. Chem. A* **2001**, *105*, 6187.
107. Baeten, A.; Maes, D. ; Geerlings, P. *J. Theoret. Biol.*, **1998**, *195*, 27.
108. Mignon, P.; Loverix, S.; Van Houtven, S.; Steyaert, J.; Geerlings, P. *in preparation*.
109. Carter, P.; Wells, J.A. *Nature*, **1988**, *332*, 565.
110. Russell, A.J.; Fersht, A.R *J. Mol. Biol*., **1987**, *193*, 803.
111. Bott, R.; Vetsch, M.; Kossiakoff, A.; Graycar, T.; Katz, B.; Power, S. *J. Biol. Chem.*, **1988**, *263*, 7895 .
112 Fersht, A. *Enzyme Structure and Mechanism*, New York, W.H. Freeman and Co., 1985.
113. Wells, J.A.; Estell, D.A. *TIBS*, **1988**, *13*, 291 (1988).

114. Geerlings, P.; De Proft, F.; Langenaeker, W. Editors, *Density Functional Theory: a Bridge between Chemistry and Physics*, Proceedings of a Two Day Symposium at the VUB, May 14-15, 1998, VUB-Press, Brussels, 1999.